Table 3 Queries and consensus-building using the Delphi method

No.	Query	Result of vote
	Definition	
1	Lymphatic vessel invasion is defined as invasion of tumour cells into lymphatic vessels	Agreement (100%)
2	Blood vessel invasion is defined as invasion of tumour cells into blood vessels	Agreement (100%)
	Assessment of BLI	
1	Scanning at 4× magnification should be used to identify suspected lesion. Then further assessment should be made at higher magnification	Agreement (87.5%)
2	BLI should not be determined in lesions presenting desmoplastic reaction	No agreement (50.0%)
3	BLI should not be determined in lesions with spicula in the space between tumour nest and stroma	Agreement (87.5%)
4	Lymphatic fluid, macrophage or blood cells in the space between tumour nests and stroma should be determined as BLI	No agreement (50.0%)
5	A tumour cluster with space around the cluster, but with vague periphery should not be determined as BLI	No agreement (25.0%)
6	Assessment of BLI should be performed in the invasive front of tumour	No agreement (50.0%)
7	Assessment of BLI should be performed with largest section containing the deepest invasive area of tumour	No agreement (50.0%)
	Staining for assessment of BLI	
1	Histochemical staining for assessment of blood vessel invasion should be performed with a whole section from the largest slice containing the deepest invasive area of the tumour	No agreement (50.0%)
2	Histochemical staining for assessment of blood vessel invasion should be performed with a section representative of the tumour	No agreement (25.0%)
3	Immunohistochemical staining for assessment of blood vessel invasion should be performed with a whole section from the largest slice containing the deepest invasive area of the tumour	No agreement (50.0%)
4	Histochemical staining for assessment of blood vessel invasion should be performed with a section representative of the tumour	No agreement (25.0%)
	Assessment of blood vessel invasion	
1	Elastica-stained internal elastic membrane without space around the tumour cluster should be determined as blood vessel invasion	Agreement (87.5%)
2	Elastica-stained internal elastic membrane without vascular endothelium around the tumour cluster should be determined as blood vessel invasion	Agreement (87.5%)
3	In elastica staining, thick arteries surrounded by the tumour cluster should be identified. If elastica-stained internal elastic membrane covering more than half of the circumference surrounding the tumour cluster is observed, the lesion should be diagnosed as blood vessel invasion	Agreement (87.5%)
4	Even without the presence of arteries, if elastica-stained internal elastic membrane covering more than half of the circumference surrounding the tumour cluster is observed, the lesion should be determined as blood vessel invasion	Agreement (87.5%)
5	Elastica-stained internal elastic membrane covering more than half of the circumference surrounding the tumour cluster without other vascular structure (ie, smooth muscle) is determined as blood vessel invasion	Agreement (87.5%)
6	Elastica-stained internal elastic membrane covering more than half of the circumference surrounding the tumour cluster without endothelial cells in H&E staining should not be determined as blood vessel invasion	No agreement (12.5%)
7	Tumour invasion into the elastica-stained vessel should be determined as blood vessel invasion	Agreement (100%)
8	Elastica-stained internal elastic membrane not covering the circumference surrounding the tumour cluster should not be determined as blood vessel invasion	No agreement (12.5%)
	Assessment of lymphatic vessel invasion	
1	An indistinguishable lesion should not be determined as lymphatic vessel invasion	Agreement (100%)
2	A tumour extending along Auerbach's neural plexus should not be determined as lymphatic vessel invasion	No agreement (75.0%)
3	A lumen with mucin should not be determined as a lymphatic vessel in case of mucinous carcinoma	No agreement (37.5%)
4	Lymphatic vessel invasion should not be determined in a lesion with small cancer cell cluster and desmoplastic reaction	No agreement (50.0%)
5	Small vessels indistinguishable between lymphatic and blood vessels should be determined as lymphatic vessel, if a thick vascular wall cannot be identified	No agreement (50.0%)
6	D2-40 positive vessel should be interpreted as lymphatic vessel regardless of the presence of endothelium	No agreement (37.5%)
7	D2-40 positive vessel without endothelium should not be interpreted as lymphatic vessel	No agreement (12.5%)
8	D2-40 negative vessel suspected as a lymphatic vessel in H&E staining should be interpreted as lymphatic vessel	No agreement (37.5%)
9	D2-40 positive cells covering all of the circumference surrounding the tumour cluster is the requirement for lymphatic vessel invasion	No agreement (0%)
10	D2-40 positive cells covering more than half of the circumference surrounding the tumour cluster is the requirement for lymphatic vessel invasion	No agreement (62.5%)
11	D2-40 positive endothelial cells covering all of the circumference surrounding the tumour cluster is the requirement for lymphatic vessel invasion	No agreement (0%)
12	D2-40 positive endothelial cells covering more than half of the circumference surrounding the tumour cluster is the requirement for lymphatic vessel invasion	Agreement (87.5%)
13	Tumour invasion into the D2-40- stained vessel is determined as lymphatic vessel invasion	Agreement (100%)

BLI, blood and lymphatic vessel invasion.

more consistent diagnosis. Pathological assessment is generally inexpensive and is available at many hospitals. So introducing a standardised pathological diagnosis can be a major contribution to current medical practice. So far, poor agreement has been reported on BLI diagnosis in many organs and conducting a multicentre study using BLI may be difficult. There are some criteria suggested by pathologists on vascular invasion and some of them were incorporated into our criterion.[23 24] While findings of H&E-stained slides should be further reviewed to search for findings with high concordance, developing objective criteria based only on H&E staining may be difficult. BLI and many pathological diagnoses are based on multiple associated histological findings. Therefore, investigation of the concordance in the histological findings associated with the diagnosis of BLI in our

Table 4 Current practice of pathological assessment at the department of pathology in different medical institutions in 2003

Institution	A	B	C	D	E	F	G	H
Number of cases	233	98	62	127	203	232	54	441
Number of colon cancer cases (%)	169 (72.5)	50 (51.0)	46 (74.2)	91 (71.7)	116 (57.1)	137 (59.1)	29 (53.7)	254 (57.6)
Number of rectal cancer cases (%)	64 (27.5)	48 (49.0)	16 (25.8)	36 (28.3	87 (42.9)	95 (40.9)	25 (46.3)	187 (42.4)
Male patients (%)	145 (62.2)	59 (60.2)	35 (56.5	68 (53.5	133 (65.5)	130 (56.0)	29 (53.7	262 (59.4)
Female patients (%)	88 (37.8)	39 (39.8)	27 (43.5)	59 (46.5)	70 (34.5	102 (44.0	25 (46.3)	179 (40.6)
Average age	65.0	64.2	67.4	68.0	63.4	64.3	64.4	63
Average number of blocks	20.1	34.4	4.8	6.4	8.8	18.0	6.3	8.0
Use of histochemical stainings	Some cases	All cases	None	Some cases	All cases	All cases	None	All cases
Range of histochemical stainings	Representative one block	All blocks	None	Representative one block	Blocks from largest slice of tumour	Representative one block	None	Representative one block
Use of immunohistochemical stainings	Some cases	None	None	Some cases	Some cases	Some cases	None	None
Antibody used in immunohistochemical stainings	D2-40	None	None	D2-40	D2-40, SMA	D2-40	None	None

framework was an important step. And the problem of diagnostic threshold or retraction artefacts remains unsolved and may be one of the reasons for poor concordance.[9] Elastica- staining and D2-40 staining have been reported to be useful in detecting BLI but may not always be associated with the detection of patients with higher risk.[14 25] Review of histochemical and immunohistochemical findings in this study suggested key findings with high concordance which may improve the quality of pathological diagnosis. Although the use of these stains alone may be insufficient, it can be used in combination with diagnostic criterion. D2-40 immunostaining was seen in lymphatic endothelium and in fibroblasts. D2-40-positive endothelial cells (but not D2-40 positive cells) was another important finding with high concordance.[26] Although histological variation was reported in blood vessel invasion, elastica-stained internal elastic membrane is the most important feature having consistent results.[27] Careful attention should be paid, however, to the lesion such as myenteric plexus ganglia invasion mimicking blood vessel invasion so as not to misdiagnose as blood vessel invasion in H&E staining. Use of some additional markers may be beneficial to reduce misdiagnosis of BLI without D2-40 expression or internal elastic membrane in the future.

Most pathological criteria to date have been developed through an informal approach by group experts in various scientific committees. A more standardised approach needs to be taken to develop pathological criteria to be used in all kinds of clinical or pathological settings. By analysing the current practice of pathologists and using the Delphi method, we have developed a framework for a new pathological diagnostic criterion. Although it still may not be sufficient to be used in multicentre trials, significant improvement over current practice is expected. We invite other pathologists' comment for its further revision and refinement. Routine elastica staining is low in cost and can be easily adopted by pathologists at different sites.[28] The applications of the present study's criterion to the daily diagnosis of BLI will likely result in the accumulation of more consistent results regarding blood vessel invasion. Although routine use of our criteria of lymphatic vessel invasion may not be feasible for advanced CRC where multiple immunostaining is required for the assessment, it may be useful for endoscopically resected pT1 CRC which is small in size and only few blocks are required.[29] The present report gives a set of criteria hopefully allowing a more consistent identification and reporting of BLI in CRC, and gives a template for the development of such diagnostic criteria that can be used in other areas of diagnostic pathology. Based on the framework that we propose, a more objective and consensus-based pathological diagnostic system can be created in many areas of diagnostic pathology.

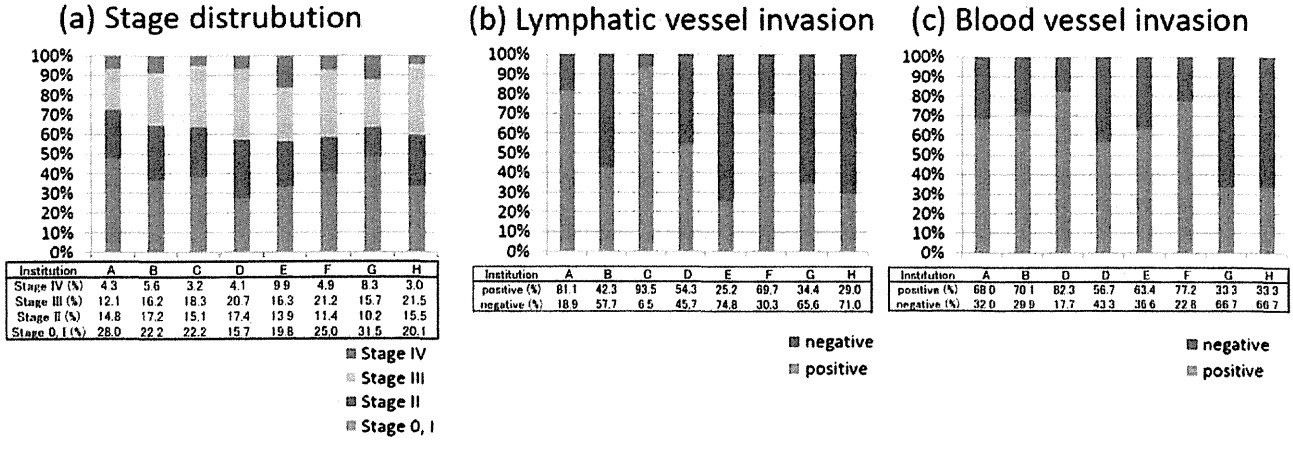

Figure 3 (A) Stage distribution of 1450 surgically resected colorectal cancer (CRC) cases among eight hospitals. (B) Distribution of positive cases of lymphatic vessel invasion among 1450 surgically resected CRC cases from eight hospitals. (C) Distribution of positive cases of blood vessel invasion among 1450 surgically resected CRC cases from eight hospitals.

Box 1 Established diagnostic criterion of blood and lymphatic vessel invasion (BLI) in Japanese society for cancer of the colon and rectum (JSSCR)

Definition

Lymphatic vessel invasion is defined as invasion of tumour cells into lymphatic vessels.

Blood vessel invasion is defined as invasion of tumour cells into blood vessels.

Assessment

Scanning at 4× magnification should be used to identify the suspected lesion. Then, further assessment should be made at higher magnification.

BLI should not be determined in lesions presenting spicula between the tumour nest and stroma.

Assessment of lymphatic vessel invasion

D2-40 positive vessel invasion should be determined as lymphatic vessel invasion, and the presence of D2-40 positive endothelial cells covering more than half of the circumference surrounding the tumour cluster should be the basis for diagnosis.

An indistinguishable lesion should not be determined as lymphatic vessel invasion.

Blood vessel invasion

In elastica staining, thick arteries surrounded by the tumour cluster should be identified. If elastica-stained internal elastic membrane covering more than half of the circumference surrounding the tumour cluster is present, the lesion should be diagnosed as blood vessel invasion.

Elastica positive vessel invasion should be determined as blood vessel invasion, and the presence of elastic-stained internal elastic membrane covering more than half of the circumference surrounding the tumour cluster should be the basis for diagnosis.

When the presence of elastica-stained internal elastic membrane covering more than half of the circumference surrounding the tumour cluster is identified, the lesion should be diagnosed as blood vessel invasion, even in the absence of accompanying artery, vascular structure or space.

Take home messages

- Current practice of pathology assessment was varied among institutions in Japan.
- Concordance was low for the pathological diagnosis of blood and lymphatic vessel invasion (BLI) in colorectal cancer, and was not any better when histochemical/immunohistochemical staining was provided.
- All histological findings associated with BLI from H&E staining were poor in agreement. However, observation of elastica-stained internal elastic membrane covering more than half of the circumference surrounding the tumour cluster as well as the presence of D2-40-stained endothelial cells covering more than half of the circumference surrounding the tumour cluster showed high concordance.
- Based on this observation, we developed a framework for pathological diagnostic criterion, using the Delphi method, which may serve as the basis for creating a standardised procedure for pathological diagnosis.

Author affiliations
[1]Pathology Division, Research Center for Innovative Oncology, National Cancer Center Hospital East, Kashiwa,Chiba, Japan
[2]Department of Pathology, National Defence Medical College, Saitama, Japan
[3]Department of Diagnostic Pathology, Kurume University Hospital, Kurume, Fukuoka, Japan
[4]Department of Pathology, Kurume University School of Medicine, Kurume, Fukuoka, Japan
[5]Department of Pathology, Kyorin University Graduate School of Medicine, Tokyo, Japan
[6]Department of Pathology, Tokyo Metropolitan Komagome Hospital, Tokyo, Japan
[7]Division of Organ Pathology, Department Microbiology and Pathology, Faculty of Medicine Tottori University, Tottori, Japan
[8]Pathology Division, National Cancer Center Hospital, Tokyo, Japan
[9]Department of Pathology, Graduate School of Medicine and Dental Sciences, Niigata University, Niigata, Japan
[10]Clinical Trial Section, Research Center for Innovative Oncology, National Cancer Center Hospital East, Chiba, Japan

Acknowledgements The authors thank Sachiko Fukuda for her excellent technical assistance. We also thank Yoshiko Ohnuma and Motoko Suzaki for their secretarial help with the consensus meetings and the distribution of the slides. We also thank Mari Kanai and Yuri Kitayama for excellent English support.

Contributors Conception and design: MK, SN and AO. Administrative support: MK and AO. Collection and assembly of data: MK, SN and AO. Data analysis and interpretation: All authors. Manuscript writing: All authors. Final approval of manuscript: All authors

Funding This work was supported by the Japanese Society for Cancer of the Colon and Rectum (JSCCR).

Competing interests None.

Ethics approval This study was approved by the local research ethics committee of the National Cancer Center Hospital (No. 2010-100).

Provenance and peer review Not commissioned; externally peer reviewed.

REFERENCES

1 Brown CE, Warren S. Visceral metastasis from rectal carcinoma. *Surg Gynecol Obstet* 1938;66:611–21.
2 Compton CC, Fielding LP, Burgart LJ, *et al*. Prognostic factors in colorectal cancer. *Arch Pathol Lab Med* 2000;124:979–94.
3 Sobin LH, Wittekind CH *TNM classification of malignant tumors*. 5th edn. New York, USA: Wiley-Liss, 1997.
4 Sobin LH, Gospodarowicz MK, Wittekind CH, eds. *TNM classification of malignant tumors*. 7th edn. New York, USA: Wiley Blackwell, Inc., 2009.
5 Dotan E, Cohen SJ. Challenges in the management of stage II colon cancer. *Semin Oncol* 2011;38:511–20.
6 Newland RC, Dent OF, Chapuis PH, *et al*. Survival after curative resection of lymph node negative colorectal carcinoma. A prospective study of 910 patients. *Cancer* 1995;76:564–71.
7 Akishima-Fukasawa Y, Ishikawa Y, Akasaka Y, *et al*. Histopathological predictors of regional lymph node metastasis at the invasive front in early colorectal cancer. *Histopathology* 2011;59:470–81.
8 Hoda SA, Hoda RS, Merlin S, *et al*. Issues relating to lymphovascular invasion in breast carcinoma. *Adv Anat Pathol* 2006;13:308–15.
9 Harris EI, Lewin DN, Wang HL, *et al*. Lymphovascular invasion in colorectal cancer: an interobserver variability study. *Am J Surg Pathol* 2008;32:1816–21.
10 Fan L, Mac MT, Frishberg DP, *et al*. Interobserver and intraobserver variability in evaluating vascular invasion in hepatocellular carcinoma. *J Gastroenterol Hepatol* 2010;25:1556–61.
11 Walgenbach-Bruenagel G, Tolba RH, Varnai AD, *et al*. Detection of lymphatic invasion in early stage primary colorectal cancer with the monoclonal antibody D2-40. *Eur Surg Res* 2006;38:438–44.
12 Yamauchi C, Hasebe T, Iwasaki M, *et al*. Accurate assessment of lymph vessel tumor emboli in invasive ductal carcinoma of the breast according to tumor areas, and their prognostic significance. *Hum Pathol* 2007;38:247–59.
13 Kawaura K, Fujii S, Murata Y, *et al*. The lymphatic infiltration identified by D2-40 monoclonal antibody predicts lymph node metastasis in submucosal invasive colorectal cancer. *Pathobiology* 2007;74:328–35.

14 Ito M, Moriya T, Ishida T, *et al*. Significance of pathological evaluation for lymphatic vessel invasion in invasive breast cancer. *Breast Cancer* 2007;14:381–7.
15 Roxburgh CS, McMillan DC, Anderson JH, *et al*. Elastica staining for venous invasion results in superior prediction of cancer-specific survival in colorectal cancer. *Ann Surg* 2010;252:989–97.
16 Powell C. The Delphi technique: myths and realities. *J Adv Nurs* 2003;41:376–82.
17 Dirschmid KW, Sterlacci W, Oellig F, *et al*. Absence of extramural venous invasion is an excellent predictor of metastasis-free survival in colorectal carcinoma stage II—a study using tangential tissue sectioning. *J Clin Pathol* 2012;65:619–23.
18 Klimstra DS, Modlin IR, Adsay NV, *et al*. Pathology reporting of neuroendocrine tumors: application of the Delphic consensus process to the development of a minimum pathology data set. *Am J Surg Pathol* 2010;34:300–13.
19 Mahler DA, Selecky PA, Harrod CG, *et al*. American College of Chest Physicians consensus statement on the management of dyspnea in patients with advanced lung or heart disease. *Chest* 2010;137:674–91.
20 Zafar SY, Currow DC, Cherny N, *et al*. Consensus-based standards for best supportive care in clinical trials in advanced cancer. *Lancet Oncol* 2012;13:e77–82.
21 Chen B, Seel L. A macro to calculate kappa statistics for categorizations by multiple raters. *In Proceeding of the 30th Annual SAS Users Group International Conference 2005*. http://www2.sas.com/proceedings/sugi30/155-30.pdf (accessed 26 Oct 2011).
22 Sejben I, Bori R, Cserni G. Venous invasion demonstrated by orcein staining of colorectal carcinoma specimens is associated with the development of distant metastasis. *J Clin Pathol* 2010;63:575–8.
23 Minsky B, Mies C. The clinical significance of vascular invasion in colorectal cancer. *Dis Colon Rectum* 1989;32:794–803.
24 Talbot IC, Ritchie S, Leighton M, *et al*. Invasion of veins by carcinoma of rectum: method of detection, histological features and significance. *Histopathology* 1981;5:141–63.
25 Messenger DE, Driman DK, McLeod RS, *et al*. Current practice patterns among pathologists in the assessment of venous invasion in colorectal cancer. *J Clin Pathol* 2011;64:983–89.
26 Kawase A, Ishii G, Nagai K, *et al*. Podoplanin expression by cancer associated fibroblasts predicts poor prognosis of lung adenocarcinoma. *Int J Cancer* 2008;123:1053–9.
27 Sato T, Ueno H, Mochizuki H, *et al*. Objective criteria for the grading of venous invasion in colorectal cancer. *Am J Surg Pathol* 2010;34:454–62.
28 Abdulkader M, Abdulla K, Rakha E, *et al*. Routine elastic staining assists detection of vascular invasion in colorectal cancer. *Histopathology* 2006;49:487–92.
29 Nivatvongs S, Rojanasakul A, Reiman HM, *et al*. The risk of lymph node metastasis in colorectal polyps with invasive adenocarcinoma. *Dis Colon Rectum* 1991;34:323–8.

PLOS | ONE

Human Subperitoneal Fibroblast and Cancer Cell Interaction Creates Microenvironment That Enhances Tumor Progression and Metastasis

Motohiro Kojima[1☯], Youichi Higuchi[1☯], Mitsuru Yokota[2], Genichiro Ishii[1], Norio Saito[2], Kazuhiko Aoyagi[3], Hiroki Sasaki[3], Atsushi Ochiai[1]*

1 Pathology Division, Research Center for Innovative Oncology, National Cancer Center Hospital East, Kashiwa, Chiba, Japan, **2** Colorectal and Pelvic Surgery Division, National Cancer Center Hospital East, Kashiwa, Chiba, Japan, **3** Genetic Division, National Cancer Center Research Institute, Chuo-ku, Tokyo, Japan

Abstract

Backgrounds: Peritoneal invasion in colon cancer is an important prognostic factor. Peritoneal invasion can be objectively identified as periotoneal elastic laminal invasion (ELI) by using elastica stain, and the cancer microenvironment formed by the peritoneal invasion (CMPI) can also be observed. Cases with ELI more frequently show distant metastasis and recurrence. Therefore, CMPI may represent a particular milieu that facilitates tumor progression. Pathological and biological investigations into CMPI may shed light on this possibly distinctive cancer microenvironment.

Methods: We analyzed area-specific tissue microarrays to determine the pathological features of CMPI, and propagated subperitoneal fibroblasts (SPFs) and submucosal fibroblasts (SMFs) from human colonic tissue. Biological characteristics and results of gene expression profile analyses were compared to better understand the peritoneal invasion of colon cancer and how this may form a special microenvironment through the interaction with SPFs. Mouse xenograft tumors, derived by co-injection of cancer cells with either SPFs or SMFs, were established to evaluate their active role on tumor progression and metastasis.

Results: We found that fibrosis with alpha smooth muscle actin (α-SMA) expression was a significant pathological feature of CMPI. The differences in proliferation and gene expression profile analyses suggested SPFs and SMFs were distinct populations, and that SPFs were characterized by a higher expressions of extracellular matrix (ECM)-associated genes. Furthermore, compared with SMFs, SPFs showed more variable alteration in gene expressions after cancer-cell-conditioned medium stimulation. Gene ontology analysis revealed that SPFs-specific upregulated genes were enriched by actin-binding or contractile-associated genes including α-SMA encoding ACTA2. Mouse xenograft tumors derived by co-injection of cancer cells with SPFs showed enhancement of tumor growth, metastasis, and capacity for tumor formation compared to those derived from co-injection with cancer cells and SMFs.

Conclusions: CMPI is a special microenvironment, and interaction of SPFs and cancer cells within CMPI promote tumor growth and metastasis.

Citation: Kojima M, Higuchi Y, Yokota M, Ishii G, Saito N, et al. (2014) Human Subperitoneal Fibroblast and Cancer Cell Interaction Creates Microenvironment That Enhances Tumor Progression and Metastasis. PLoS ONE 9(2): e88018. doi:10.1371/journal.pone.0088018

Editor: Soroku Yagihashi, Hirosaki University Graduate School of Medicine, Japan

Received September 27, 2013; **Accepted** January 2, 2014; **Published** February 4, 2014

Funding: This work was supported by JSPS KAKENHI grant number 24590458, and a grant of a 3rd-term Comprehensive 10-year Strategy for Cancer Control (23-A-3). The funders had no role in study design, data collection and analysis, decision to publish, or preparation of the manuscript.

Competing Interests: The authors have declared that no competing interests exist.

* E-mail: aochiai@east.ncc.go.jp

☯ These authors contributed equally to this work.

Introduction

Although tumor size is a major prognostic factor in many cancers, prognosis in gastrointestinal cancer is stratified not by tumor size but by tumor spread [1]. Peritoneal invasion in colorectal cancer has been reported to be a strong prognostic factor, but this term was not well defined, and detection and diagnosis methods have been questioned [2–4]. Recent pathological reports have demonstrated that elastica stain, which highlights the peritoneal elastic lamina near the periotoneal surface, is useful for objective detection of peritoneal invasion. We and others have determined that peritoneal invasion defined as tumor invasion beyond the peritoneal elastic lamina (elastic laminal invasion: ELI) is a strong prognostic factor that can influence future pT criteria in the Union for International Cancer Control (UICC) TNM classification [5–7]. The peritoneum is a very thin membrane, within 500 μm thick, and the peritoneal elastic lamina exists within this membrane. The frequency of synchronous metastasis and recurrence is increased by 2 to 4 times when a tumor invades this narrow space [5]. These results may suggest that tumor progression and metastasis are facilitated by a cancer microenvironment formed by peritoneal invasion (CMPI). The extent of

CMPI can be identified by using elastica stain, and pathological features of CMPI can also be determined.

A tissue microarray facilitates the evaluation of protein expression for a large number of tissue blocks from a single specimen, and area-specific tissue microarrays have been reported to be useful for studying specific tumor areas in large cohorts [8]. After determination of CMPI by using elastica stain, a tissue core can be obtained from this area and a comparison with the features of other tumor areas can also be performed. This process may allow for an assessment of the important biological phenomena occurring in this cancer microenvironment.

Recent advances in cancer research have established the concept of cancer microenvironment that promotes tumor initiation, invasion, and metastasis [9]. Although the cancer microenvironment is composed of many types of cells, the use of area-specific tissue microarrays may allow for a focus on the cell components that characterize CMPI. Furthermore, if these cell components can be cultivated from the histologically corresponding subperitoneal region, a biological study to elucidate this putative cancer-promoting microenvironment can be performed.

The aim of this study was to explain how the colorectal cancer prognosis is affected by peritoneal invasion. We constructed area-specific tissue microarray system to determine the characteristic cell components of CMPI. Next, we cultivated specific fibroblast subpopulations from the submucosal and subperitoneal layers of the human colonic wall. The biological characteristics and gene profiles of submucosal fibroblasts (SMFs) and subperitoneal fibroblasts (SPFs) with or without cancer-cell-conditioned medium (CCCM) stimulation were compared. Subsequently, we constructed xenograft tumors by co-injection of cancer cells with either SPFs or SMFs. Our study proposed a new candidate for a cancer-promoting microenvironment in colon cancer and elucidated SPFs as crucial players in the enhancement of tumor progression and metastasis.

Patients and Methods

Ethics Statement

This study was approved by the National Cancer Center Hospital East Institutional Review Board (No: 19-021). A written general consent to use biologic materials for research was obtained from each participant prior to tissue acquisition. Animal experiments were approved by the Animal Ethics Committee of the National Cancer Center Hospital East (K11-032).

Patient Characteristics and Detection of ELI

Four hundred consecutive patients with TNM classification (5th edition) pT3 and pT4a colon cancer [10], undergoing surgery between 1996 and 2003 at the National Cancer Center Hospital East, were enrolled. Using elastica stain, we identified 173 cases with ELI and further examined these using area-specific tissue microarrays [5,8]. Of the 173 cases with ELI, 107 were pT3 and 66 were pT4a.

Construction of Area-Specific Tissue Microarrays

To elucidate the pathological features of CMPI in colon cancer tissue, we defined the cancer microenvironment as follows: (a) CMPI has a tumor border with peritoneal invasion and (b) the cancer microenvironment formed by submucosal invasion (CMSI) has a submucosal invasive tumor border (Figure 1A) [5]. The 2-point tissue microarray was then established as previously described [8]. Each tumor area was marked with ink on the histological slide; a single tissue core of 2 mm in diameter was obtained from each cancer microenvironment and transferred to a recipient block using a Tissue Microarrayer (Azumaya, Tokyo, Japan). In 24 cases, insufficient cancer tissue was obtained from the CMPI. However, sufficient tissue was obtained in 149 cases; these were analyzed histologically and immunohistochemically (See Materials and Methods S1, and Table S1).

Antibodies, Regents, and Immunohistochemistry

The antibodies, reagents, and the immunohistochemical procedures used are described in Materials and Methods S1 and the Table S2.

Evaluation of Area-Specific Tissue Microarray Sections

High-resolution slide images were acquired from all tissue cores with hematoxylin-eosin (H.E) and immunohistochemistry staining, using NanoZoomer 2.0-HT slide scanner (Hamamatsu photonics, Hamamatsu, Japan). All cores were examined using viewer software (NDP view: Hamamatsu photonics, Hamamatsu, Japan). When the area of fibrosis exceeded 50% of a whole tissue core with a 2 mm diameter upon H.E staining, it was defined as positive for marked fibrosis. On immunohistochemical staining, hot spots with CD3-, CD31-, and CD68-positive cells or vessels were selected in the viewer software, then an image of x20 magnification (0.51 mm^2) was taken, and saved as a JPEG file. Positive cells or vessels were counted in each image using morphometric software (WinRoof, Mitani Corporation, Fukui, Japan). Moreover, the area with highest alpha smooth muscle actin (α-SMA) expression in fibroblasts was selected, then a x20 magnification (0.51 mm^2) image was taken, and saved as a JPEG file. The ratio of the α-SMA positive area in the image was calculated using morphometric software, as described previously [11]. The α-SMA expression in normal muscle tissue, as determined by comparison with a serial H.E slide, was not evaluated. H.E and immunohistochemical staining data of CMPI was compared with that of CMSI to elucidate the histological characteristics of CMPI.

Primary Cells and Cell Lines

Submucosal tissue was obtained from sigmoid colon tissue more than 5 cm distant from the tumor. Colonic tissue was dissected from the muscular layer on the luminal side, and lamina propria and mucosal layer tissues were obtained. Next, the lamina propria was scrubbed away to obtain submucosal tissue. Subperitoneal tissue was obtained from the sigmoid colon mesentery at more than 5 cm distant from the tumor by using operating tweezers and scissors. These tissues were washed with phosphate-buffered saline (PBS) and incubated in 5% trypsin for 20 minutes, 3 times. The supernatant was centrifuged, plated on a dish, and submucosal fibroblasts (SMFs) and subperitoneal fibroblasts (SPFs) were obtained and then grown and maintained in MF-medium (Toyobo, Tokyo, Japan) [12]. All experiments were performed on cells within 8 passages.

The human colorectal cancer cell lines DLD-1 and Caco-2 were obtained from the American Type Culture Collection and grown in Dulbecco's modified Eagle medium (DMEM) (Sigma-Aldrich, Saint Louis, MO) containing 100 U/mL penicillin, 100 μg/mL streptomycin (Sigma-Aldrich, Saint Louis, MO), and 10% fetal bovine serum (FBS; Gibco, Palo Alto, CA).

Cell Proliferation Assay, Immunocytochemical Staining, and Flow Cytometry Analysis

Cell proliferation assays, immunocytochemical staining, and flow cytometry analyses were performed as described in Materials and Methods S1.

Stimulation of Fibroblasts by Cancer Cell Medium

Initially, $1.7\times10^4/cm^2$ of fibroblasts and DLD-1 cells were grown separately in DMEM containing 100 U/mL penicillin, 100 μg/mL streptomycin, and 10% FBS for 48 hours, and then were starved for 24 hours. Next, the medium was removed from the fibroblasts, and the medium from the starved DLD-1 cells was added to the fibroblasts for 24 hours to establish fibroblasts with cancer-cell-conditioned medium (CCCM) stimulation. As control, fibroblasts were starved for 48 hours (yielding fibroblasts without CCCM). SPFs and SMFs either with or without CCCM were assessed by using immunocytochemistry or gene expression analysis. As for the evaluation of immunocytochemical α-SMA expression, the area with highest α-SMA expression was selected, then a x20 magnification ($0.51\ mm^2$) image was taken, and saved as a JPEG file. The ratio of α-SMA positive area in the image was calculated using morphometric software (WinRoof, Mitani Corporation, Fukui, Japan).

Gene Expression Analysis using Microarray

Three sets of SPFs and SMFs, either with or without CCCM, obtained from 3 different patients, were used in this study. We used GeneChip Human Genome U133 Plus 2.0 arrays (Affymetrix, Santa Clara, CA). Target cDNA was generated from 100 ng of total RNA extracted from each sample using a 3′ IVT Express Kit (Affymetrix, Santa Clara, CA). The procedures for target hybridization, washing and staining for signal amplification were performed according to the supplier's protocols. The arrays were scanned with a Gene Chip Scanner 3000 (Affymetrix, Santa Clara, CA), and the intensity of each feature of the array was calculated by using GeneChip Operating Software, version 1.1.1 (Affymetrix, Santa Clara, CA). The average intensity was standardized to the target intensity, which was set equal to 1000, to reliably compare different arrays. The values were log transformed and median centered. The programs GeneSpring (Agilent Technologies, Santa Clara, CA) and Excel (Microsoft Corporation, Redmond, WA) were used to perform the numerical analyses for gene selection.

Xenograft Transplantation and Tumor Formation Assay

Either 1×10^6 human colorectal cancer cells Caco-2 or DLD-1 alone, or with either 1×10^6 SPFs or SMFs, were injected subcutaneously (s.c.) into the back of SCID mice (8- 12 weeks of age; CLEA, Tokyo, Japan). Tumor volumes were calculated weekly as described previously [13]. Mice injected with Caco-2 alone or with either SPFs or SMFs were killed after 10 weeks, and those injected with DLD-1 alone or with either SPFs or SMFs were killed after 8 weeks, and tumor weights were evaluated. For distant metastatic analysis, lung and liver tissue was removed and fixed in 10% formalin, and for the analysis of lymph node metastasis, neck and inguinal adipose tissue was also removed and fixed; all tissues were histologically examined. We used 8 mice in each group.

To elucidate the capacity of fibroblasts to enhance tumor formation, serial dilutions of Caco-2 or DLD-1 cancer cells were similarly co-injected with either 1×10^6 SMFs or SPFs. Tumor formation was evaluated 4 weeks after the injection. We used 4 mice for each group.

Statistical Analysis

X^2 test and Student's t test were used in the tissue microarray analysis, cell proliferation assay, xenograft transplantation, and tumor formation assay. A $P<0.05$ was defined as statistically significant. In the microarray analysis, gene expression data were analyzed using GeneSpring GX12 (Agilent Technologies, Santa Clara, CA). Row data were summarized by using MAS5 and normalized by log transformation and median centering for numerical analyses for gene selection. For principal component analysis (PCA), we used probe sets that were reliably measured and varied by 3-fold above the global median in at least 2 samples (approximately 10%); analyses were performed using GeneSpring GX12. The differentially expressed probe sets used in supervised hierarchical clustering were selected based on $P<0.05$ and fold change (FC) >2.0. P values were calculated using one way ANOVA with Benjamini and Hochberg FDR multiple testing correction. Hierarchical clustering with weight-average linkage clustering was performed using Cluster and Treeview programs (Michael Eisen, Stanford University, genome-www.stanford.edu). The functional annotation clustering of Gene Ontology Enrichment analysis was performed using DAVID software, with the classification stringency set to "High", and the significant clusters were selected based on an enrichment score >2.0 and a $P<0.01$ (Fisher's exact test after Benjamini and Hochberg FDR multiple testing correction) [14,15].

Results

Histological Features of ELI

Not only tumor cells, but also varieties of stromal cells constitute a distinct cancer microenvironment, and some promote tumor metastasis [9]. First, we elucidated the significant histological features of CMPI to shed light on phenomena occurring in this milieu by using area-specific tissue microarrays. The clinicopathological features of the 149 cases used are shown in Table S1. On H.E staining, we found extensive fibrosis (over 50%) more frequently in CMPI than was seen in CMSI (Figure 1B). The ratio of α-SMA positive area in CMPI was also higher than that seen in CMSI (Figure 1C). The proportions of T lymphocytes, macrophages, or microvessels evaluated using CD3, CD68, or CD31, respectively, were not significantly different between CMPI and CMSI (Figure 1D–F). Both in CMPI and CMSI, plump spindle-shaped fibroblasts were major source of α-SMA expression, and the ratio was successfully analyzed by using morphometric software (Figure 2A–D). Considering our previous results, which indicated that peritoneal invasion defined by ELI was closely associated with distant metastasis, we hypothesized that fibroblasts in the subperitoneal layer could be implicated not only in prominent fibrosis and activation, but also in the tumor's progression and metastasis. We then decided to isolate fibroblasts from the subperitoneal layer that histologically corresponded to peritoneal invasion. Fibroblasts from the submucosal layer were used as controls..

Isolation and Characterization of Cultured Human SPFs and SMFs

At first, we evaluated the morphological and biological characteristics of SPFs and SMFs in a normal state. Both cultured human SPFs and SMFs showed similar spindle-shaped morphologic characteristics (Figure S1A–B). SPFs and SMFs from 3 patients could be cultured over 10 passages, except for 1 SPF case (data not shown). Immunocytochemistry and flow cytometry revealed the obtained SPFs and SMFs were consistent with fibroblasts (Figure S1C–D). We found weak α-SMA expression in a few SPFs and SMFs. The doubling time for SPFs and SMFs was 79.9 hours and 36.3 hours, respectively, and the growth of SMFs was faster than that of SPFs ($P<0.05$), which suggested a biological difference between SPFs and SMFs (Figure S1E).

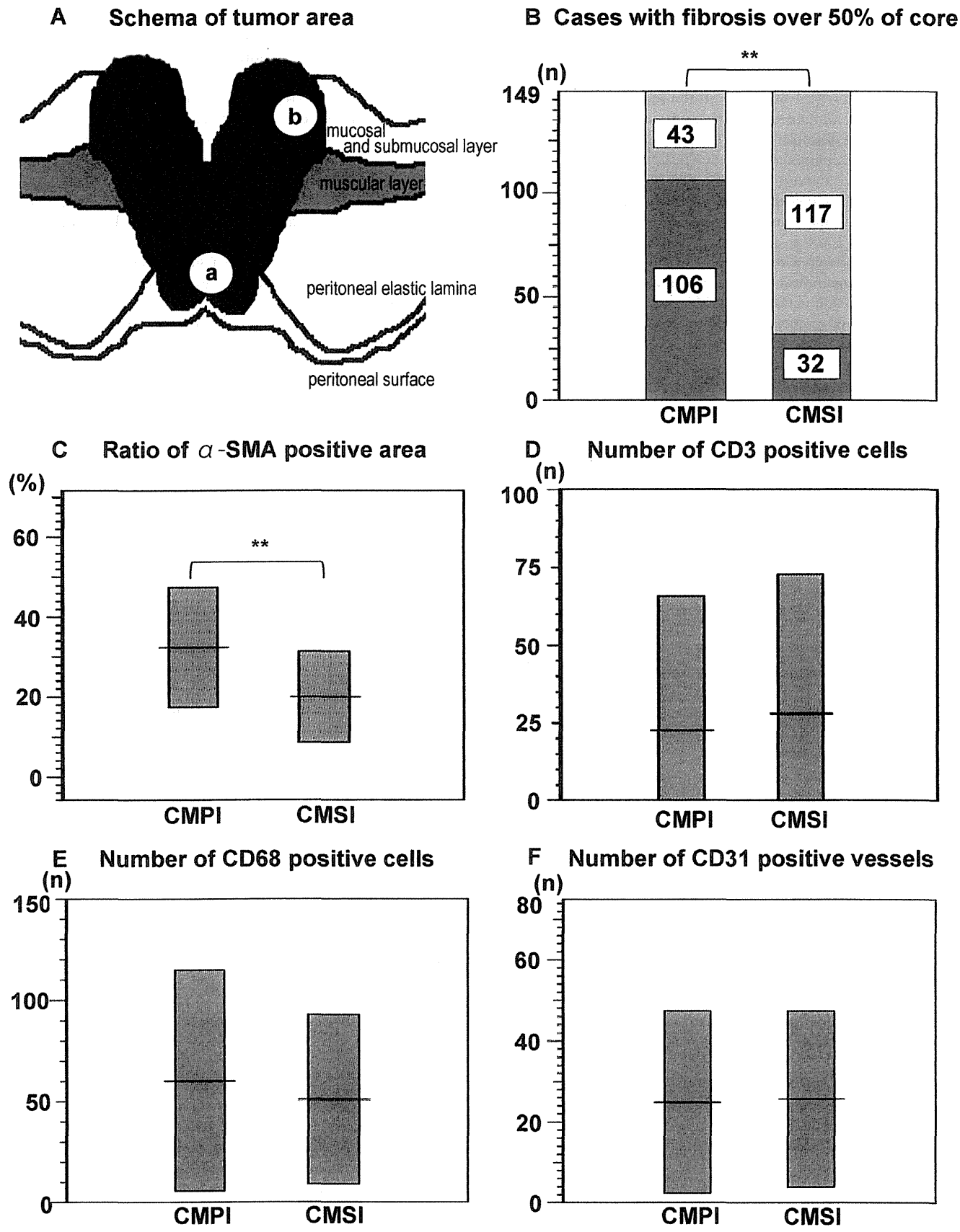

Figure 1. Pathological features of tumor microenvironment explored by using area-specific tissue microarray. (A) Schema of the cancer microenvironment formed by peritoneal invasion (CMPI) and the cancer microenvironment formed by submucosal invasion (CMSI) defined as

(a) invasive front with peritoneal invasion and (b) submucosal invasive front, respectively. (B) The distribution of fibrosis in human colon cancer tissue. Dark gray bars show the number of the cases with fibrosis over 50% of the core from each tumor area, and light gray bars show the number of the cases without extensive fibrosis. Core samples with CMPI showed a higher frequency of marked fibrosis than did core samples with CMSI ($P<0.01$). (C) Distribution of α-SMA expression in human colon cancer tissue. CMPI showed higher α-SMA expressions than those seen in CMSI ($P<0.01$). (D) Distribution of CD3-positive cells in human colon cancer tissue. Numbers of CD3-positive cells were not significantly different between CMPI and CMSI. (E) Distribution of CD68-positive cells in human colon cancer tissue. Numbers of CD68-positive cells were not significantly different between CMPI and CMSI. (F) Distribution of CD31-positive vessels in human colon cancer tissue. Numbers of the CD31-positive vessels were not significantly different between CMPI and CMSI. Results in (B) are presented by case numbers, and those in (C–F) are presented as the mean ± SD of 149 cases (**$P<0.01$).

doi:10.1371/journal.pone.0088018.g001

Gene Expression Profiling Comparison between SPFs and SMFs

To assess the phenotypical differences between SPFs and SMFs, the gene expression profiles of fibroblasts with or without CCCM stimulation were compared. PCA revealed 4 distinct clusters, depending on their origin and CCCM stimulation, which overcame the individual variation (Figure 3A and B). Supervised cluster analysis also revealed 4 distinct clusters (Figure 3C). This indicated the phenotypical difference in fibroblasts within the colonic wall. And this difference depended on the histoanatomical location. Furthermore, the reaction to CCCM stimulation was also different.

Next, we compared gene expression profiles in these fibroblasts with and without CCCM stimulation, separately (Figure 3D–E). Data from SPFs without CCCM stimulation were enriched by the gene ontology (GO) terms "extracellular matrix" and "proteinaceous extracellular matrix", which formed annotation cluster 1. Major expracellular matrix (ECM) components of collagens (COL1A1, COL4A1, COL4A2, COL5A1, and COL16A1), laminin, or fibronectin were included in this cluster. Moreover, gene expression related to components that bind to the ECM was also upregulated in SPFs and formed annotation cluster 2. Annotation cluster 3 was enriched for GO terms associated with "granules" or "vesicles" (Figure 3D and Table S3). This result suggested the gene expression profile associated with basic function in fibroblasts is different between SPFs and SMFs within the colonic wall. The top 20 genes highly expressed in SPFs also included several ECM components. Genes associated with fibrogenesis or the myofibroblastic differentiation of FLI1 and NOX4 were also found in the top 20 genes (Table S4). Among other highly expressed genes in SPFs without CCCM stimulation, we found POSN, SPARC, or COL4A1, which are known to be highly expressed in the cancer stroma; and many of these are prognostic factors [11,16,17].

Most of the genes with increased expressions in SPFs without CCCM stimulation were also retained in the presence of CCCM stimulation; however, there were some differences (Figure 3D–E, Table S5–6). In GO analysis of SPFs with CCCM stimulation, the order of annotation clusters were changed compared to that seen in SPFs without CCCM stimulation. Among the top 20 genes, 13 genes were conserved and 7 genes were replaced. These results suggest a difference in the reaction to CCCM stimulation between SPFs and SMFs. The existence of SPFs-specific genes that are upregulated after CCCM stimulation was estimated.

We then analyzed these genes to establish the biological characteristics of SPFs after exposure to CCCM. A Venn diagram revealed 193 upregulated genes in SPFs and 59 in SMFs after CCCM stimulation. Of these, 51 were commonly upregulated both in SPFs and SMFs, 142 were SPFs specific, and only 8 were SMFs specific (Figure 4A). We then also focused on downregulated genes, and discovered 215 in SPFs and 146 in SMFs. Of these, 138 were commonly downregulated both in SPFs and SMFs, 77 were SPFs specific, and only 8 were SMFs specific (Figure 4B). These results suggested that SPFs showed more variable alteration in gene expression after CCCM stimulation. GO term analysis of SPF-specific genes downregulated after CCCM stimulation did not revealed any annotation cluster over 3.0 of the enrichment score (data not shown). In contrast, GO term analysis of SPFs-specific genes upregulated after CCCM stimulation revealed that terms such as "actin binding", "cytoskeletal binding protein", "contractile fiber", "LIM domain", "contractile fiber part", "sarcomere", and "myofibril" formed annotation cluster 1–3 (Figure 4C). Most of these genes were known to be related to cell contraction. Among the top 20 genes were many cytoskeletal or contractility associated genes. Surprisingly, ACTA2 that encodes α-SMA was upregulated specifically in SPFs after CCCM stimulation (Figure 4D). This result was confirmed by immunocytochemistry (Figure 4E–F). Morphometric analysis in immunocytochemical expression revealed that α-SMA expression was upregulated specifically and significantly in SPFs after CCCM stimulation in protein level (Figure S2, $P<0.05$). Variable upregulation and downregulation of genes after CCCM stimulation was a significant feature in SPFs. ACTA2 encoding α-SMA was included in this SPFs-specific upregulated gene set. Cancer associated fibroblasts (CAFs) include α-SMA-positive activated myofibroblasts. Together with the result of area-specific tissue microarrays, marked α-SMA expression in CMPI is depended on the sensitive character of SPFs which may associated with the difference in cancer microenvironment.

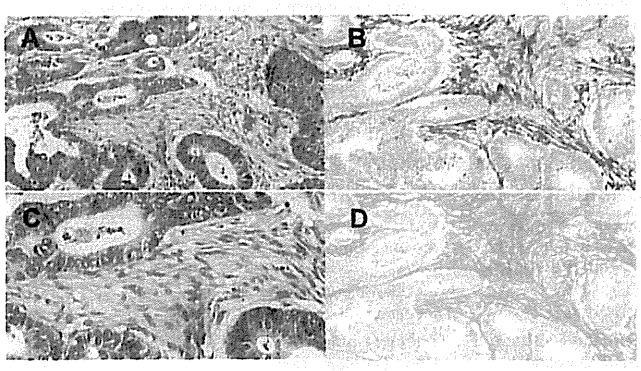

Figure 2. Histological features of fibrosis in the cancer microenvironment formed by peritoneal invasion (CMPI). (A) Histological features of stromal component of CMPI. Both in CMPI and the cancer microenvironment formed by submucosal invasion (CMSI), plump spindle-shaped fibroblasts were major sources of the stroma. (B) Marked α-SMA expression was found in fibroblasts. (C) Higher magnification more clearly revealed plump spindle-shaped fibroblasts. (D) Using morphometric software, we successfully detected and analyzed α-SMA expression.

doi:10.1371/journal.pone.0088018.g002

SPFs Enhance Tumor Growth, Metastasis and Tumor Formation Ability more Strongly than do SMFs

To elucidate the functional differences of fibroblasts in the colonic wall, we injected human colorectal cancer cell lines Caco-2

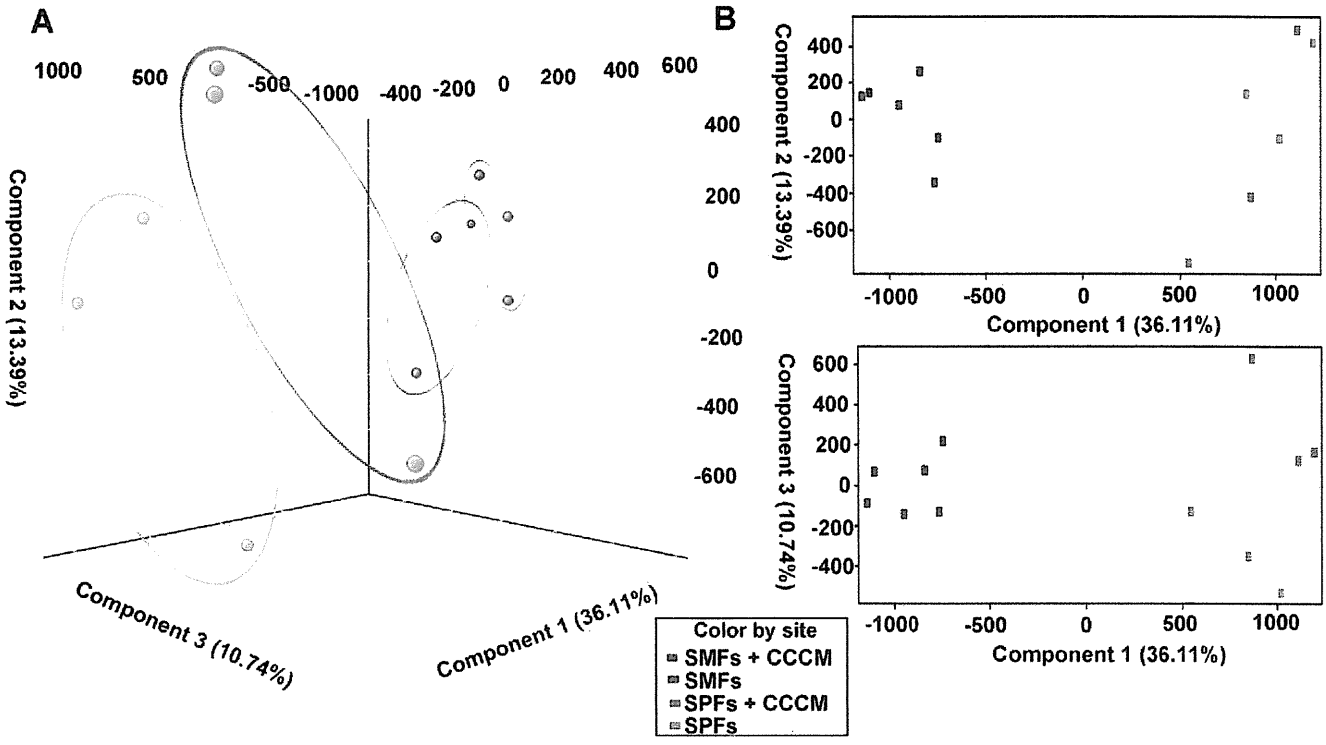

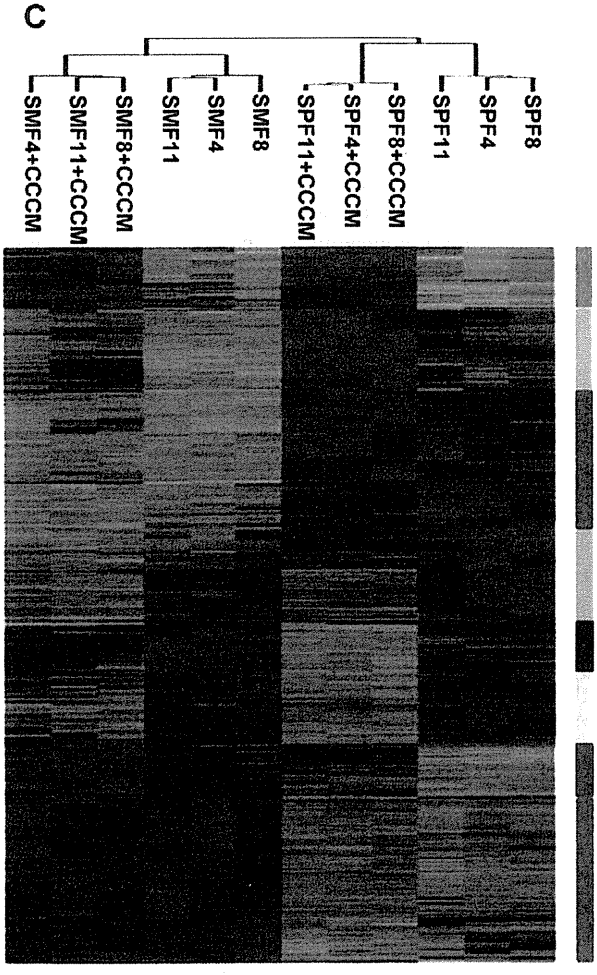

D

Upregulated gene clusters in SPFs compared with SMFs

Annotation Cluster 1	Enrichment Score: 9.31	
Gene Ontology ID	Gene Ontology Term	*P* value
GO:0031012	extracellular matrix	<.01
GO:0005578	proteinaceous extracellular matrix	<.01
SP_PIR_KEYWORDS	extracellular matrix	<.01
Annotation Cluster 2	Enrichment Score: 3.92	
Gene Ontology ID	Gene Ontology Term	*P* value
GO:0030247	polysaccharide binding	<.01
GO:0001871	pattern binding	<.01
GO:0005539	glycosaminoglycan binding	0.02
GO:0030246	carbohydrate binding	0.05
Annotation Cluster 3	Enrichment Score: 3.92	
Gene Ontology ID	Gene Ontology Term	*P* value
GO:0031093	platelet alpha granule lumen	<.01
GO:0060205	cytoplasmic membrane-bounded vesicle lumen	<.01
GO:0031983	vesicle lumen	<.01
GO:0031091	platelet alpha granule	<.01
GO:0030141	secretory granule	0.09
GO:0044433	cytoplasmic vesicle part	0.29

E

Upregulated gene clusters in SPFs with CCCM stimulation compared with SMFs with CCCM stimulation

Annotation Cluster 1	Enrichment Score: 10.12	
Gene Ontology ID	Gene Ontology Term	*P* value
SP_PIR_KEYWORDS	extracellular matrix	<.01
GO:0031012	extracellular matrix	<.01
GO:0005578	proteinaceous extracellular matrix	<.01
Annotation Cluster 2	Enrichment Score: 4.92	
Gene Ontology ID	Gene Ontology Term	*P* value
GO:0016477	cell migration	<.01
GO:0048870	cell motility	<.01
GO:0051674	localization of cell	<.01
Annotation Cluster 3	Enrichment Score: 4.66	
Gene Ontology ID	Gene Ontology Term	*P* value
GO:0001871	pattern binding	<.01
GO:0030247	polysaccharide binding	<.01
GO:0005539	glycosaminoglycan binding	<.01
GO:0030246	carbohydrate binding	0.11

Figure 3. Gene expression profiles in subperitoneal fibroblasts (SPFs) and submucosal fibroblasts (SMFs) with and without cancer-cell-conditioned medium (CCCM) stimulation. (A) Red is the microarray profile in SMFs with CCCM stimulation, blue is SMFs without CCCM stimulation, green is SPFs with CCCM stimulation, and silver is SPFs without CCCM stimulation. Three-dimensional representation of principal component analysis (PCA) component 1, 2, and 3. (B) Two dimensional representation of PCA components 1 and 2 (upper), and PCA components 1 and 3 (lower). Fibroblasts formed independent clusters, depending on histoanatomical site and the presence of CCCM stimulation. (C) Supervised cluster analysis in fibroblasts also revealed distinct clusters depending on histoanatomical site and the presence of CCCM stimulation. (D) Gene ontology analysis of upregulated genes in SPFs compared with SMFs. (E) Gene ontology analysis of genes upregulated in SPFs with CCCM stimulation, compared with SMFs with CCCM stimulation. Most of the genes with increased expressions in SPFs were retained after CCCM stimulation; however, there were some differences, and the order of annotation clusters were changed after CCCM stimulation.
doi:10.1371/journal.pone.0088018.g003

or DLD-1 s.c., alone, or along with either SPFs or SMFs, into SCID mice. At 7 weeks after the injection, all mice demonstrated tumor formation. The growth of tumors arising from cancer cells injected along with SPFs grew faster than that arising from the injection of cancer cells alone or co-injection with SMFs (Figure 5A). The final weights of tumors arising from cancer cells co-injected with SPFs were also larger than those arising from the injection of cancer cells alone or from co-injection with SMFs

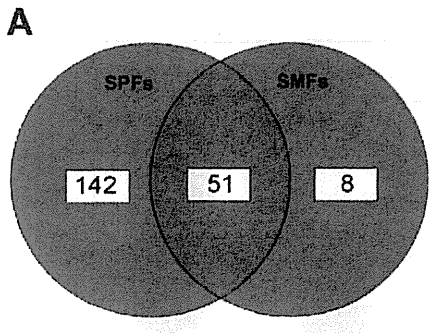

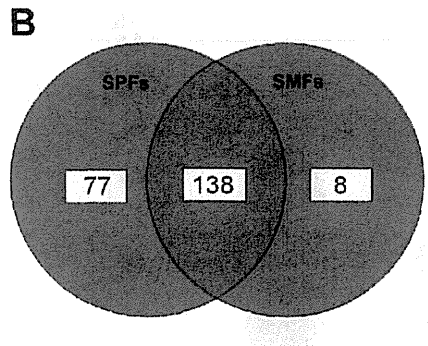

C SPFs specific upregulated gene cluster after CCCM stimulation

Annotation Cluster 1	Enrichment Score: 4.73	
Gene Ontology ID	Gene Ontology Term	*P* value
GO:0003779	actin binding	< .01
SP_PIR_KEYWORDS	actin-binding	< .01
GO:0008092	cytoskeletal protein binding	0.01
Annotation Cluster 2	Enrichment Score: 3.97	
Gene Ontology ID	Gene Ontology Term	*P* value
SP_PIR_KEYWORDS	LIM domain	< .01
INTERPRO	IPR001781:Zinc finger, LIM-type	< .01
SMART	SM00132:LIM	< .01
Annotation Cluster 3	Enrichment Score: 3.84	
Gene Ontology ID	Gene Ontology Term	*P* value
GO:0044449	contractile fiber part	< .01
GO:0043292	contractile fiber	< .01
GO:0030017	sarcomere	< .01
GO:0030016	myofibril	< .01

D Top 20 in SPFs specifically upregulated genes after CCCM stimulation

Probe Set ID	*P* value	FC	Gene Symbol
206029_at	< .01	13.41	ANKRD1
206825_at	< .01	10.84	OXTR
205795_at	< .01	8.67	NRXN3
210511_s_at	< .01	8.09	INHBA
204671_s_at	< .01	7.66	ANKRD6
212473_s_at	< .01	7.57	MICAL2
202628_s_at	< .01	6.96	SERPINE1
229669_at	< .01	6.75	LOC100507263
201195_s_at	< .01	6.61	SLC7A5
200974_at	< .01	6.52	ACTA2
205518_s_at	< .01	6.49	CMAH
217452_s_at	< .01	6.32	B3GALT2
205442_at	< .01	6.21	MFAP3L
1558828_s_at	< .01	6.2	LOC728264
223063_at	< .01	5.84	C1orf198
204589_at	< .01	5.59	NUAK1
226869_at	< .01	5.44	MEGF6
213067_at	< .01	5.43	MYH10
203432_at	< .01	5.14	TMPO
206117_at	< .01	5.09	TPM1

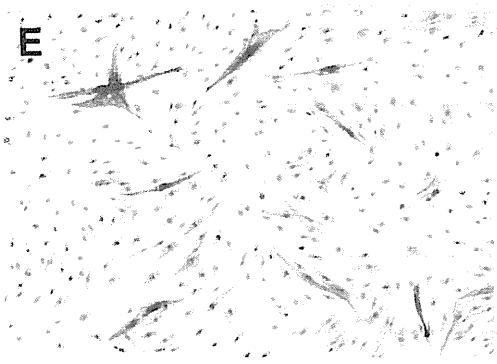

Figure 4. Gene modification in subperitoneal fibroblasts (SPFs) after cancer-cell-conditioned medium (CCCM) stimulation. (A) Genes upregulated by CCCM stimulation. (B) Genes downregulated by CCCM stimulation. (C) Top 3 annotation clusters in gene ontology analysis of SPFs-specific genes upregulated by CCCM stimulation. (D) Top 20 genes upregulated specifically in SPFs after CCCM stimulation. (E) Immunocytochemical α-SMA expression in SMFs after CCCM stimulation. (F) Immunocytochemical α-SMA expression in SPFs after CCCM stimulation. α-SMA expression was upregulated specifically in SPFs after CCCM stimulation (see also Figure S2).
doi:10.1371/journal.pone.0088018.g004

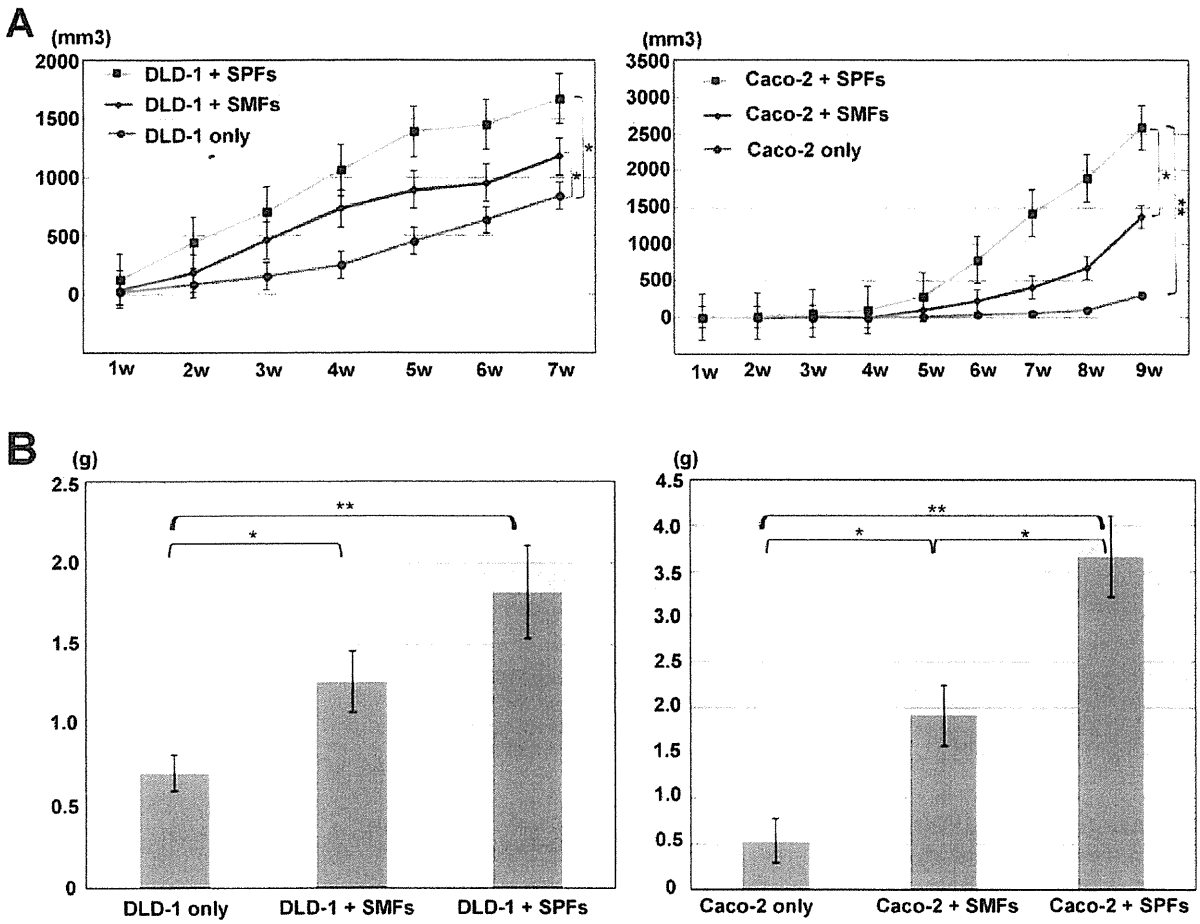

C

	Liver metastasis	Lung metastasis	Lymph node
Caco-2 + SPFs (10 weeks)	0/8	0/8	0/8
Caco-2 + SMFs (10 weeks)	0/8	0/8	0/8
DLD-1 + SPFs (8 weeks)	0/8	0/8	**4/8**
DLD-1 + SMFs (8 weeks)	0/8	0/8	**2/8**

D

Cells inoculated	Number of cancer cells	Tumor formation rate
Caco-2 only	1×10^6	0/4
Caco-2 + SPFs (1×10^6)	1×10^6	4/4
Caco-2 + SMFs (1×10^6)	1×10^6	4/4
Caco-2 only	5×10^5	0/4
Caco-2 + SPFs (1×10^6)	5×10^5	4/4
Caco-2 + SMFs (1×10^6)	5×10^5	4/4
Caco-2 only	1×10^5	0/4
Caco-2 + SPFs (1×10^6)	1×10^5	4/4
Caco-2 + SMFs (1×10^6)	1×10^5	3/4
Caco-2 only	5×10^4	0/4
Caco-2 + SPFs (1×10^6)	5×10^4	2/4
Caco-2 + SMFs (1×10^6)	5×10^4	0/4

Cells inoculated	Number of cancer cells	Tumor formation rate
DLD-1 only	1×10^6	3/4
DLD-1 + SPFs (1×10^6)	1×10^6	4/4
DLD-1 + SMFs (1×10^6)	1×10^6	4/4
DLD-1 only	5×10^5	1/4
DLD-1 + SPFs (1×10^6)	5×10^5	4/4
DLD-1 + SMFs (1×10^6)	5×10^5	4/4
DLD-1 only	1×10^5	0/4
DLD-1 + SPFs (1×10^6)	1×10^5	4/4
DLD-1 + SMFs (1×10^6)	1×10^5	1/4
DLD-1 only	5×10^4	0/4
DLD-1 + SPFs (1×10^6)	5×10^4	3/4
DLD-1 + SMFs (1×10^6)	5×10^4	1/4

Figure 5. Subperitoneal fibroblasts (SPFs) actively contribute to cancer progression. (A, left) Xenograft tumor growth in mice injected with DLD-1 human colorectal cancer cells alone (blue line, 840.7±112.6 mm^3 in 7 weeks), co-injected with DLD-1 cells and submucosal fibroblasts (SMFs; red line, 1178.0±177.6 mm^3 in 7 weeks), and co-injected with DLD-1 cells and subperitoneal fibroblasts (SPFs; green line, 1672.8±214.7 mm^3 in 7 weeks). The differences of tumor volume between DLD-1 cells alone and DLD-1 cells with SPFs, and between DLD-1 cells alone and DLD-1 cells with SMFs were statistically significant ($P<0.05$). (A, right) Xenograft tumor growth in mice injected with Caco-2 human colorectal cancer cells alone (blue line, 308.6±127.7 mm^3 in 9 weeks), co-injected with Caco-2 cells and SMFs (red line, 1363.1±284.3 mm^3 in 9 weeks), and co-injected with Caco-2 and SPFs (green line, 2595.1±349.5 mm^3 in 9 weeks). The differences of tumor volume between Caco-2 cells alone and Caco-2 cells with SPFs ($P<$

0.01), and between Caco-2 cells with SMFs and Caco-2 cells with SPFs ($P<0.05$) were statistically significant. Xenograft tumors derived from co-injection of cancer cells and SPFs grew faster than those derived from injection of cancer cells alone, or co-injection of cancer cells and SMFs. (B, left) Xenograft tumor weight in mice injected with DLD-1 cells alone was 0.71±0.11 g, co-injected with DLD-1 cells and SMFs was 1.27±0.19 g, and co-injected with DLD-1 cells and SPFs was 1.82±0.28 g in 8 weeks. The differences of tumor weight between DLD-1 cells alone and DLD-1 cells with SPFs ($P<0.01$), and between DLD-1 cells alone and DLD-1 cells with SMFs ($P<0.05$) were statistically significant. (B, right) Xenograft tumor weight in mice injected with Caco-2 cells alone was 0.53±0.24 g, co-injected with Caco-2 cells and SMFs was 1.91±0.34 g, and co-injected with Caco-2 cells and SPFs was 3.66±0.45 g in 10 weeks. The differences of tumor weight between DLD-1 cells alone and DLD-1 cells with SPFs ($P<0.01$), between DLD-1 cells alone and DLD-1 cells with SMFs ($P<0.05$), and between DLD-1 cells with SPFs and DLD-1 cells with SMFs ($P<0.05$) were statistically significant. Weights of xenograft tumors derived from co-injection of cancer cells with SPFs were higher than those of tumors derived from injection of cancer cells alone, or co-injection of cancer cells and SMFs (left: DLD-1, right: Caco-2). (C) Although the value did not reach statistical significance, xenograft tumors derived from co-injection of DLD-1 cells and SPFs showed twice the frequency of lymph node metastasis (n = 4) compared to those deriving from co-injection of DLD-1 cells and SMFs (n = 2). (D) Co-injection of cancer cells and SPFs result in enhanced tumor formation capacity. Results are presented as the mean ± SE of 8 mice (*$P<0.05$. **$P<0.01$).
doi:10.1371/journal.pone.0088018.g005

(Figure 5B). Although the difference was not statistically significant, tumors arising from the co-injection of DLD-1 cells with SPFs more frequently resulted in lymph node metastasis than did those formed from the co-injection of DLD-1 cells with SMFs (Figure 5C).

Next, the cancer cells being injected were serially diluted and tumor formation was evaluated at 4 weeks after the injection, as described previously [13]. Comparison with mice injected with cancer cells alone or co-injected with cancer cells and SMFs, enhanced tumor formation was found in mice co-injected with cancer cells and SPFs, and tumor formation was observed even when the injected cells were diluted to 5×10^4 (Caco-2) or 1×10^4 (DLD-1). These results suggested that SPFs enhanced tumor growth, metastasis, and tumor formation capacity, in comparison with the effect of SMFs; these findings may be related to the peritoneal invasion dependent clinical outcome in colon cancer.

Discussion

Fibroblasts are one of the most common types of stromal cells in connective tissue. Fibroblasts and loose connective tissue, which is one morphological type of connective tissue, are present throughout the body and contribute to the maintenance of the structural framework of most tissues, including the gastrointestinal tract [18]. Histologically, the gastrointestinal tract is composed of 5 layers that consist of the lamina propria, submucosa, muscular layer, subserosa, and serosa. Loose connective tissue and fibroblasts exist in every layer and have distinct physiological and pathological functions [19,20].

SPFs are known to produce peritoneal fluid and facilitate appropriate functioning of intra-abdominal organs [21]. Previous reports have shown that the marked contractile ability in SPFs was implicated in the colonic strictures in Crohn's disease [22,23]. In the field of peritoneal dialysis, SPFs have been reported to produce growth factors, cytokines, or chemokines in response to TGF-β stimulation and have been implicated in the failure of peritoneal dialysis [24]. However, the implication of SPFs in tumor progression is not known, and our study is the first to report the contribution of SPFs in tumor progression and metastasis that is dependent on peritoneal invasion in colon cancer.

Our findings seem to support the concept of microenvironmental regulation of cancer. The tumor microenvironment consists of distinct cell types, including fibroblasts, blood cells, vascular-originated cells, and more. They synergistically create a distinct microenvironment according to tumor progression, such as the core primary tumor microenvironment, the invasive tumor microenvironment, or the metastatic tumor microenvironment [9]. Area-specific tissue microarrays were very useful to expand this concept into the pathological phenomenon and biological study was then performed based on these results. Interestingly, the fibroblasts we obtained from the submucosal and subperitoneal tissues showed biological differences dependent on the histoanatomical site. In addition, our finding of marked phenotypical modification in SPFs suggests that fibroblasts from different histoanatomical sites show different reactions to cancer stimuli. We used Caco-2 with low tumorigenic and metastatic potential and DLD-1 with a higher tumorigenic and metastatic potential in this study. DLD-1 has been known to preferentially cause lymph node metastasis rather than lung or liver metastasis, and our data is in accordance with previous reports [25–28]. Together with the xenograft tumor results in which SPFs enhanced tumor growth and tumor formation in Caco-2 and DLD-1, and promote lymph node metastasis in DLD-1, we have clarified that this fibroblastic difference is implicated in colon cancer progression that is dependent on peritoneal invasion.

In general, fibroblasts within the tumor stroma, so-called CAFs, acquired a modified phenotype. CAFs are enriched in α-SMA positive active myofibroblasts and are known to play an active role in tumor progression [29,30]. Residual fibroblasts are one of the sources of CAFs, and residual fibroblasts exposed to cancer stimulation show phenotypical modification. Although the tumor-promoting ability of CAFs has been reported to be diverse and dependent on cancer origin, intra-tumoral diversity has not been clear [31]. Our data suggests the physiological diversity of fibroblasts within one organ produces the intra-tumoral diversity of CAFs. Therefore, gene profiles in fibroblasts with and without cancer CCCM stimulation may provide new insights into their diversity in colon cancer.

We are speculating that a fibroblast subpopulation with tumor-promoting capacity can be enriched in the subperitoneal layer. Their original phenotype may include a previously reported CAFs marker, and variable gene modification in response to cancer stimuli could be a characteristic feature of tumor-promoting fibroblasts. Recently, activated proteins in CAFs have been considered to be a target of therapy [32]. However, not all kinds of CAFs may promote tumor progression [31]. Our gene expression profile data in SPFs with and without CCCM stimulation may also be useful for future stromal-target therapy. SPFs with robust tumor promotion ability showed higher gene expression associated with an ECM component, and marked gene upregulation associated with cell contraction, including α-SMA, after CCCM stimulation. Recently both stromal-cell contractile ability and ECM stiffness have been reported to influence epithelial cell migration and invasion. Also, α-SMA is one of the representative markers of CAFs and myofibroblasts, and its expression is associated with biological contractile ability. Furthermore, α-SMA expression in tumor stroma was reported to be a prognostic factor in colorectal cancer. Therefore, our result suggests the importance of mechanotransduction theory in the study of the tumor microenvironment [33–35].

From the first categorization efforts reported by Lockhart-Mummery, primary colon cancer has been consistently stratified based on the extent of its spread into the bowel wall [36]. More recent pathological investigations have revealed that peritoneal invasion is a prognostic factor, and is a candidate for discriminating high-risk stage II colon cancer, and those patients who may receive benefit from post-operative therapy [3,37,38]. We and others reported the utility of elastica stain for the objective diagnosis of peritoneal invasion. We have proven that objective identification of peritoneal invasion is also useful for investigating biological phenomena specifically occurring in this tumor microenvironment [39]. Recently, Liang et al. proposed that pT3 tumors with ELI should be subdivided into further categories like pT3b [6]. Our findings support the subdivision of cases with ELI from those without ELI, and the diversity of the fibroblasts could be one factor associated with frequent metastases in cases with ELI.

In conclusion, fibrosis with α-SMA expression is a significant feature of the cancer microenvironment formed by peritoneal invasion in human colon cancer. The biological features and functions of fibroblasts in the subperitoneal tissue are different from those in submucosal tissue, and their phenotypical modification by cancer stimuli and contribution to tumor growth and metastasis are also different. Specifically, SPFs from the subperitoneal tissue showed characteristic biological features of a marked ECM component and contractile-associated gene expression, and functions that accelerate tumor formation and metastasis. Considering these comprehensive pathological and biological data, we propose that CMPI is a special microenvironment that promotes tumor growth and metastasis. In CMPI, SPFs and cancer cells interaction play an active and crucial role in tumor progression.

Supporting Information

Figure S1 Biological characteristics of subperitoneal fibroblasts and submucosal fibroblasts. (A) Immunocytochemical staining for vimentin in SPFs. (B) Immunocytochemical staining for vimentin in SMFs. (C) Flow cytometric analysis of SPFs and SMFs. (D) Immunocytochemical staining of SPFs and SMFs. Protein expression results were positive for vimentin and CD105, and negative for an epithelial marker (AE1/3), a neural marker (S-100), mesothelial markers (calretinin, CK8), endothelial markers (CD31, 34), and lymphocyte and monocyte markers (CD3, 14, 20, 45, 68), suggesting that the obtained cells were fibroblasts. We found weak α-SMA expression in a few SPFs and SMFs. (E) Growth curve of SPFs (blue) and SMFs (red). SPFs showed significantly longer doubling time than did SMFs ($P<0.01$). Results are presented as the mean ± SE of triplicate measurements (**$P<0.01$).
(TIF)

Figure S2 Morphometric analysis of immunocytochemical α-SMA expression. α-SMA expression was upregulated specifically and significantly in SPFs after cancer-cell-conditioned medium (CCCM) stimulation. Results are presented as the mean ± SE of 3 experiments (*$P<0.05$).
(TIF)

Table S1 Patient Characteristics Entered into Area-Specific Tissue Microarray.
(DOCX)

Table S2 Primary antibodies used in this study.
(DOCX)

Table S3 Upregulated gene clusters and composing genes in SPFs compared with SMFs.
(DOCX)

Table S4 Top 20 genes in SPFs compared with SMFs.
(DOCX)

Table S5 Upregulated gene clusters in SPFs with cancer-cell-conditioned medium (CCCM) stimulation compared with SMFs with CCCM stimulation.
(DOCX)

Table S6 Top 20 upregulated genes in SPFs with cancer cell-conditioned medium (CCCM) stimulation compared with SMFs with CCCM stimulation.
(DOCX)

Materials and Methods S1 Supplementary Materials and Methods.
(DOCX)

Acknowledgments

We thank MA's Communications Inc. for their excellent English editing support.

Author Contributions

Conceived and designed the experiments: MK YH GI AO. Performed the experiments: MK YH AO. Analyzed the data: MK YH KA HS. Contributed reagents/materials/analysis tools: MY NS. Wrote the paper: MK YH AO.

References

1. Sobin LH, Gospodarowicz MK, Wittekind CH (2009) TNM Classification of Malignant Tumors, (7th edn), New York: Wiley-Blackwell, Inc. 15 p.
2. Newland RC, Dent OF, Lyttle MN, Bokey L (1994) Pathologic determinants of survival associated with colorectal cancer with lymph node metastases. A multivariate analysis of 579 patients. Cancer 73: 2076–2082.
3. Shepherd NA, Baxter KJ, Love SB (1997) The prognostic importance of peritoneal involvement in colonic cancer: a prospective evaluation. Gastroenterology 112: 1096–1102.
4. Stewart CJ, Morris M, de Boer B, Iacopetta B (2007) Identification of serosal invasion and extramural venous invasion on review of Dukes' stage B colonic carcinomas and correlation with survival. Histopathology 51: 372–378.
5. Kojima M, Nakajima K, Ishii G, Saito N, Ochiai A (2010) Peritoneal elastic laminal invasion of colorectal cancer: the diagnostic utility and clinicopathologic relationship. Am J Surg Pathol 34: 1351–1360.
6. Liang WY, Zhang WJ, Hsu CY, Arnason T, Berger D, et al. (2013) Retrospective Evaluation of Elastic Stain in the Assessment of Serosal Invasion of pT3N0 Colorectal Cancers. Am J Surg Pathol "in press".
7. Shinto E, Ueno H, Hashiguchi Y, Hase K, Tsuda H, et al. (2004) The subserosal elastic lamina: an anatomic landmark for stratifying pT3 colorectal cancer. Dis Colon Rectum 47: 467–473.
8. Shinto E, Tsuda H, Ueno H, Hashiguchi Y, Hase K, et al. (2005) Prognostic implication of laminin-5 gamma 2 chain expression in the invasive front of colorectal cancers, disclosed by area-specific four-point tissue microarrays. Lab Invest 85: 257–266.
9. Hanahan D, Weinberg RA (2011) Hallmarks of cancer: the next generation. Cell 144: 646–674.
10. Sobin LH, Wittekind CH (1997) TNM Classification of Malignant Tumors, (5th edn), New York: Wiley-Liss.
11. Tsujino T, Seshimo I, Yamamoto H, Ngan CY, Ezumi K, et al. (2007) Stromal myofibroblasts predict disease recurrence for colorectal cancer. Clin Cancer Res 13: 2082–2090.
12. Witowski J, Jorres A (2006) Peritoneal cell culture: fibroblasts. Perit Dial Int 26: 292–299.
13. Hoshino A, Ishii G, Ito T, Aoyagi K, Ohtaki Y, et al. (2011) Podoplanin-positive fibroblasts enhance lung adenocarcinoma tumor formation: podoplanin in fibroblast functions for tumor progression. Cancer Res 71: 4769–4779.
14. Huang DW, Sherman BT, Lempicki RA (2009) Systematic and integrative analysis of large gene list using DAVID bioinformatics resources. Nat Protoc 4: 44–57.

15. Huang DW, Sherman BT, Lempicki RA (2009) Bioinformatics enrichment tools: paths toward the comprehensive functional analysis of large gene lists. Nucleic Acids Res 37: 1–13.
16. Fukushima N, Kikuchi Y, Nishiyama T, Kudo A, Fukayama M (2008) Periostin deposition in the stroma of invasive and intraductal neoplasms of the pancreas. Mod Pathol 21: 1044–1053.
17. Bae YK, Kim A, Kim MK, Choi JE, Kang SH et al. (2013) Fibronectin expression in carcinoma cells correlates with tumor aggressiveness and poor clinical outcome in patients with invasive breast cancer. Hum Pathol "in press".
18. Maximow AA, Bloom W (1942). Textbook of Histology. 4th edition ed. Philadelphia: W. B. Saunders Company: 54–75.
19. Kaye GI, Lane N, Pascal RR (1968). Colonic pericryptal fibroblast sheath: replication, migration, and cytodifferentiation of a mesenchymal cell system in adult tissue. II. Fine structural aspects of normal rabbit and human colon. Gastroenterology 54: 852–865.
20. Nik AM, Reyahi A, Ponten F, Carlsson P (2013) Foxf2 in intestinal fibroblasts reduces numbers of Lgr5(+) stem cells and adenoma formation by inhibiting Wnt signaling. Gastroenterology 144: 1001–1011.
21. van der Wal JB, Jeekel J (2007) Biology of the peritoneum in normal homeostasis and after surgical trauma. Colorectal Dis 9 Suppl 2: 9–13.
22. Brannigan AE, Watson RW, Beddy D, Hurley H, Fitzpatrick JM (2002) Increased adhesion molecule expression in serosal fibroblasts isolated from patients with inflammatory bowel disease is secondary to inflammation. Ann Surg 235: 507–511.
23. Regan MC, Flavin BM, Fitzpatrick JM, O'Connell PR (2000) Stricture formation in Crohn's disease: the role of intestinal fibroblasts. Ann Surg 231: 46–50.
24. Witowski J, Thiel A, Dechend R, Dunkel K, Fouquet N (2001) Synthesis of C-X-C and C-C chemokines by human peritoneal fibroblasts: induction by macrophage-derived cytokines. Am J Pathol 158: 1441–1450.
25. Oikonomou E, Kothonidis K, Zografos G, Nasioulas G, Andrea L et al. (2007) Newly established tumorigenic primary human colon cancer cell lines are sensitive to TRAIL-induced apoptosis in vitro and in vivo. Br J Cancer 97: 73-84.
26. Kawada K, Hosogi H, Sonoshita M, Sakashita H, Manabe T et al. (2007) Chemokine receptor CXCR3 promotes colon cancer metastasis to lymph nodes. Oncogene 26: 4679–4688.
27. Céspedes MV, Espina C, Gracia-Cabezas MA, Trias M, Boluda A et al. (2007) Orthotopic microinjection of human colon cancer cells in nude mice induces tumor foci in all clinically relevant metastatic sites. Am J Pathol 170: 1077–1085.
28. de Vries JE, Dinjens WN, De Bruyne GK, Verspaget HW, van der Linden EP et al. (1995) In vivo and in vitro invasion in relation to phenotypic characteristics of human colorectal carcinoma cells. Br J Cancer 71: 271–277.
29. Polanska UM, Orimo A (2013) Carcinoma-associated fibroblasts: Non-neoplastic tumour-promoting mesenchymal cells. J Cell Physiol 2013; 228: 1651–1657.
30. Kalluri R, Zeisberg M (2006) Fibroblasts in cancer. Nat Rev Cancer 6: 392–401.
31. Erez N, Truitt M, Olson P, Arron ST, Hanahan D (2010) Cancer-associated fibroblasts are activated in in cipient neoplasia to orchestrate tumor promoting inflammation in an NF-kappaB-dependent manner. Cancer Cell 17: 135–147.
32. Brennen WN, Isaacs JT, Denmeade SR (2012) Rationale behind targeting fibroblast activation protein-expressing carcinoma-associated fibroblasts as a novel chemotherapeutic strategy. Mol Cancer Ther 11: 257–66.
33. Levental KR, Yu H, Lakins JN, Egeblad M, Erler JT, et al. (2009) Matrix crosslinking forces tumor progression by enhancing integrin signaling. Cell 139: 891–906.
34. Butcher DT, Alliston T, Weaver VM (2009) A tense situation: forcing tumor progression. Nat Rev Cancer 9: 108–122.
35. Kümper S, Marshall CJ (2011) ROCK-driven actomyosin contractility induces tissue stiffness and tumor growth. Cancer Cell 19: 695–697.
36. Lockhart-Mummery JP (1926) Two hundred cases of cancer of the rectum treated by perineal excision. British Journal of Surgery 14: 110–124.
37. Newland RC, Chapuis PH, Smyth EJ (1987) The prognostic value of substaging colorectal carcinoma. A prospective study of 1117 cases with standardized pathology. Cancer 60: 852–857.
38. Dotan E, Cohen SJ (2011) Challenges in the management of stage II colon cancer. Semin Oncol 38: 511–520.
39. Kojima M, Yokota M, Saito N, Nomura S, Ochiai A (2012) Elastic laminal invasion in colon cancer: diagnostic utility and histological features. Front Oncol "in press".

図説

大腸癌の浸潤・転移機構

Mechanism of invasion and metastasis in colorectal cancer

小嶋基寛　　落合淳志

はじめに

癌は周囲組織への浸潤に続いて遠隔組織に広がる．この現象を転移と呼ぶ．癌の転移には大きく分けて血行性，リンパ行性および播種性が存在するが，大腸癌においては循環を介した血行性とリンパ行性転移が頻度として高い(**図1**)[1]．転移成立の段階全体像を**図1**に示した．また，各段階を要約および図説すると以下のようになる．

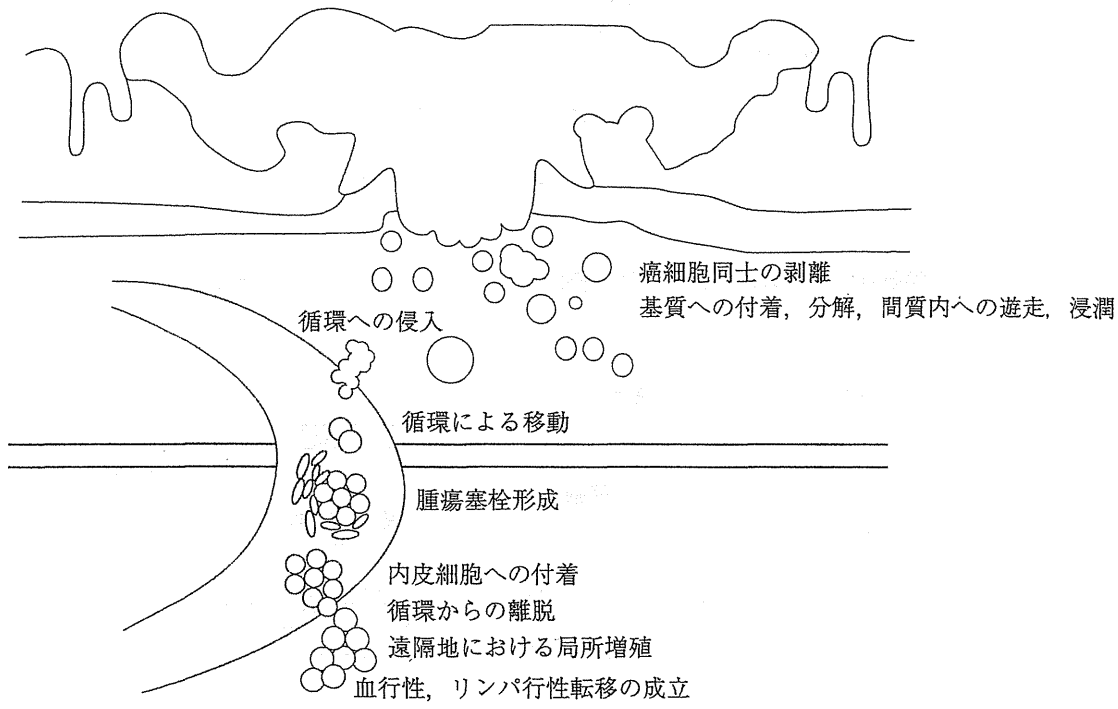

著者らの施設のStage II-IV大腸癌切除症例における同時性転移頻度

リンパ節転移	血行性転移 (肝転移)	腹膜播種
55.5%(223/402)	19.4%(78/402)	6.0%(24/402)

図1　血行性，リンパ行性転移成立の過程(文献[1]より改変)

Motohiro Kojima, Atsushi Ochiai: Pathology Division, Research Center for Innovative Oncology, National Cancer Center Hospital East　国立がん研究センター東病院 臨床開発センター 臨床腫瘍病理分野

0047-1852/14/¥60/頁/JCOPY

血行性，リンパ行性転移成立の段階

(1) 癌細胞同士の解離(**図2**).
(2) 基質の分解，間質内への遊走，浸潤，循環経路への侵入(**図2**).
(3) 循環による移動，内皮細胞への付着，循環経路からの離脱(**図3**).
(4) 遠隔臓器における局所増殖(**図3**).

各段階に多数の分子がかかわり大腸癌を含む腫瘍の複雑な浸潤・転移機構を構成しているため，その研究の多くは上記のいずれかの段階に特化されている．各段階を総論的にまとめ，大腸癌における特徴も示した．また，大腸癌における転移の各段階にかかわる主な因子を**表1**にまとめた．

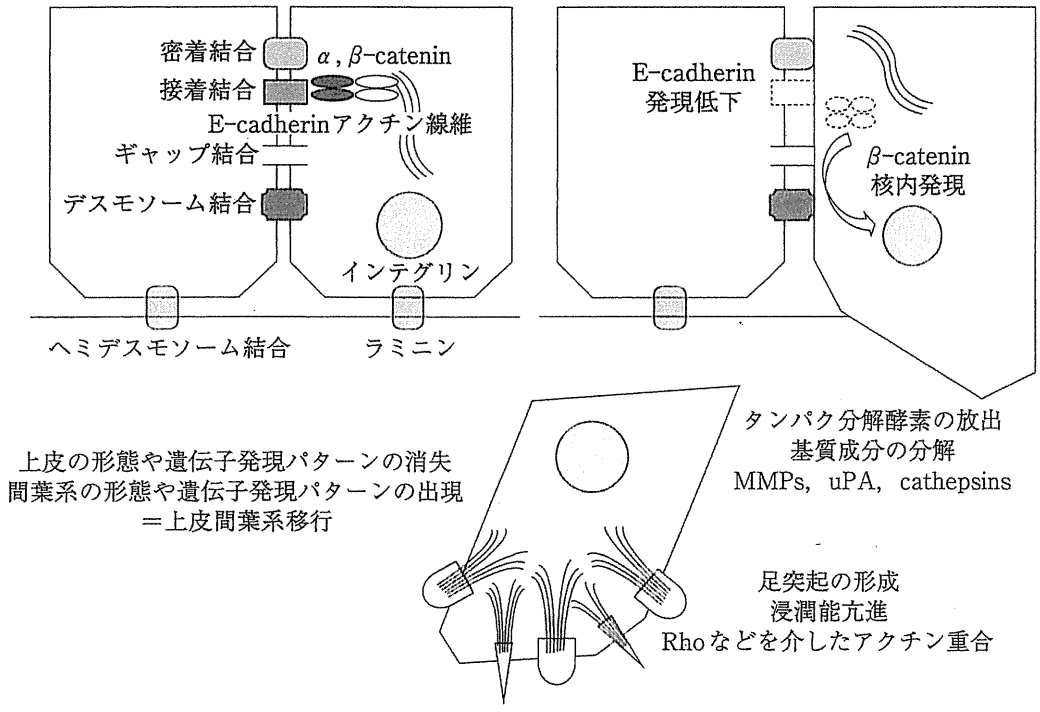

図2　癌細胞同士の剥離および基質の分解，間質内への遊走，浸潤，循環への侵入の過程

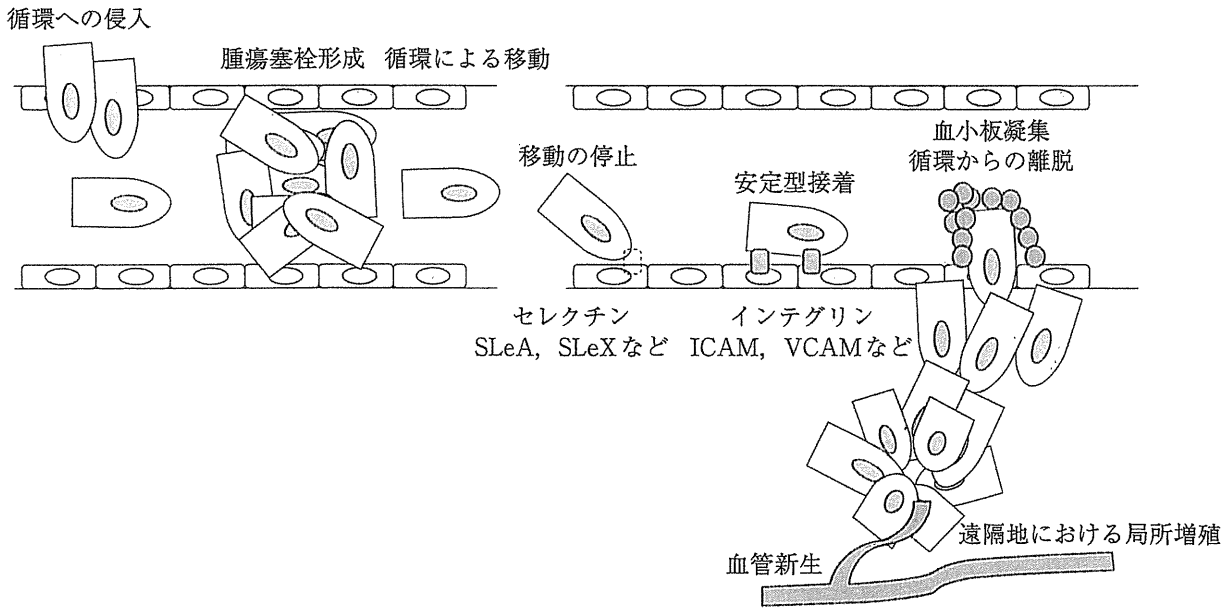

図3　循環による移動，内皮細胞への付着，循環からの離脱および遠隔地における局所増殖の過程

表1 大腸癌転移段階にかかわる分子

	かかわる分子ファミリー	大腸癌における報告
細胞同士の剥離	カテニン	α−, β−, γ−catenin
	カドヘリン	E−, N−, P−cadherin
基質の分解，間質内への遊走，浸潤	インテグリン	α6β4, αvβ5, αvβ6, β1, α2, α3, etc
循環への侵入	MMPs	MMP−2, 7, 9, 13, 14, TIMP−3, 4
循環からの離脱	uPA	
	カテプシン	cathepsin B, D
	Rhoファミリー	RhoA, Rac1, cdc42
	セレクチン	E−selectin, P−selectin
	免疫グロブリンスーパーファミリー	ICAM−1, VCAM−1
	インテグリン	
	ガレクチン	galectin 3
	TF抗原	

(文献[1]より改変)

1. 癌細胞同士の解離

生体内における細胞は細胞同士もしくは細胞と基質が接着して存在している．上皮細胞同士の接着は密着接合，接着結合，ギャップ結合，デスモソーム結合といった特殊で強固な接着構造を形成する．また上皮細胞は基底膜に接着し，ヘミデスモソームを形成する．癌進展過程における細胞同士もしくは基底膜との接着の異常や解離は転移が成立する際の最初の過程と考えられる．

大腸癌細胞における癌細胞同士の解離

大腸癌発癌過程においてβ−cateninの分解にかかわるAPC変異が非常に高頻度で観察される．これらWnt pathwayの異常は大腸癌発生に重要である．β−cateninの細胞質内発現も早期病変から認められ，接着結合において結合するE−cadherin発現低下も相関してみられる．これらの変化は癌の発生，進展に寄与していると考えられる．

2. 基質の分解，間質内への遊走，浸潤，循環への侵入

腫瘍の浸潤には基質成分の分解が必要で様々なタンパク分解酵素が知られている．ウロキナーゼ型プラスミンアクチベータ(uPA)，マトリックスメタロプロテアーゼ(MMPs)，カテプシンなどが代表的である．細胞は遊走の際，足突起を形成する．足突起においてフォーカルアドヒージョンを形成して基質と接着する．また突起を伸縮させることにより細胞自体が運動する．細胞自体には細胞の接着と運動の両者が必要不可欠である．基質と接着する際にはインテグリンなどのタンパクが重要である．一方，運動においてはアクチンとミオシンからなるストレスファイバーの形成が重要で，これはフォーカルアドヒージョンを介してインテグリンと結合している．アクチン重合，ストレスファイバーの形成や収縮にはRhoAが重要な役割を果たす．基質の分解と遊走という異なる生物学的事象が複合的に合わさって浸潤という現象は生じ，結果として癌は循環へ侵入する．

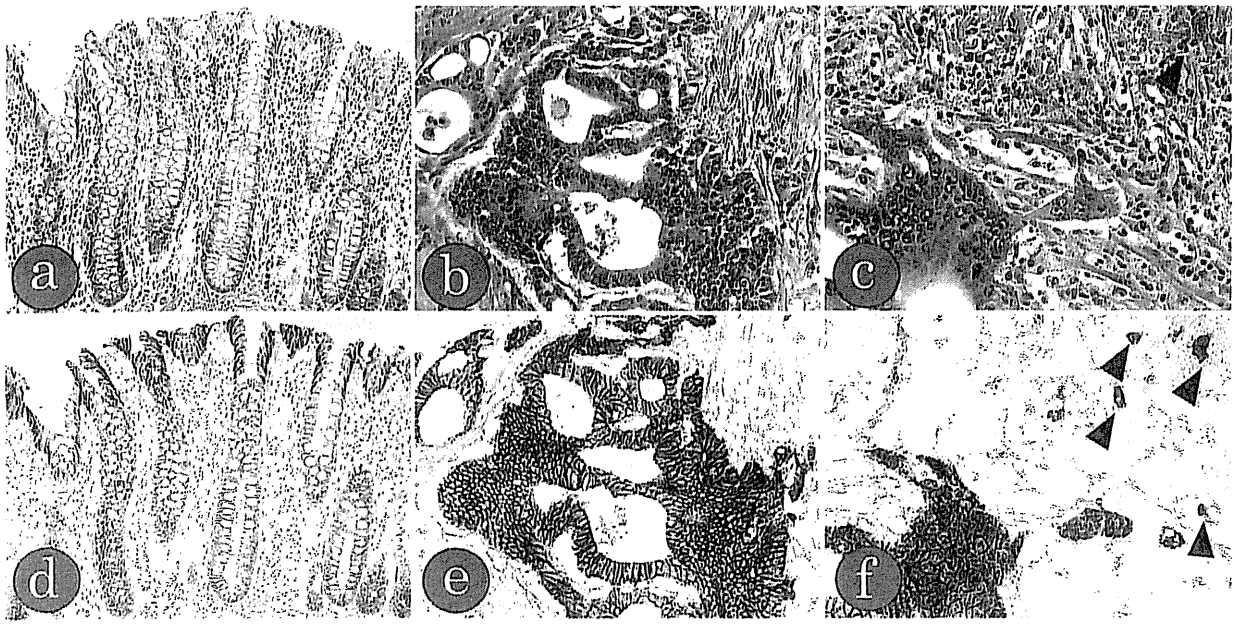

図4　大腸粘膜および大腸癌におけるβ-catenin発現局在と組織像

a, d. 正常粘膜におけるH・E染色(a)およびβ-catenin免疫染色(d). 正常粘膜におけるβ-catenin発現は細胞膜にほぼ限局してみられる.

b, e. 大腸癌非浸潤先進部のH・E染色(b)およびβ-catenin免疫染色(e). 大腸癌の非浸潤先進部におけるβ-cateninの発現は細胞膜および細胞質が中心で, 一部核にも発現がみられる.

c, f. 大腸癌浸潤先進部のH・E染色(c)およびβ-catenin免疫染色(f). 大腸癌の浸潤先進部におけるβ-cateninの発現は細胞質と核が中心である. 孤立散在性で上皮の形態が消失した腫瘍細胞胞巣(budding)が右上にみられるが(矢頭), それらにおいては細胞質と核の発現がより強く観察される.

大腸癌細胞における基質の分解, 間質内への遊走, 浸潤, 循環への侵入

Wnt pathwayの異常は引き続いて生じる浸潤の際に病理組織学的に観察されるbuddingおよび生物学的に観察される上皮-間葉移行(epithelial-mesenchymal transition: EMT)においても重要である. buddingは大腸癌浸潤先進部で観察される5個以下の腫瘍細胞胞巣を指し, buddingにおいてはβ-cateninの核内発現が非常に強く認められる. またEMTとは生物学的に上皮細胞がその特徴的な形態や遺伝子発現のパターンを捨てて, 間葉細胞に特徴的な形をとることで, E-cadherin発現低下は重要なマーカーである. 両者は共通する現象を異なる分野からとらえていると思われ, 特に大腸癌においてはbudding, EMTのいずれにおいてもWnt経路が重要であることは確かである(図4). Wnt経路の亢進は下流のMMP7を活性化する. 生物学的にMMP7発現亢進は基質の分解のみならずIGFやVEGFの活性化を介して, 血管新生を亢進させることが知られている. 病理学的にもMMP7発現亢進は大腸癌浸潤先進部に特異的にみられ, 実際のヒト組織でも生物学的現象と類似した作用が生じていると考えられる[2]. これらの現象には癌の微小環境もかかわっていると考えられる. 近年buddingは漿膜近傍で強く生じることが報告されており, EMTもコラーゲンIで誘導されることから, 癌細胞の性質のみならず, 周囲の環境との相互作用によっても, これらの現象は生じていると思われる[3].

3. 循環による移動，内皮細胞への付着，循環からの離脱

循環の環境は癌細胞の生存に厳しい環境であると思われる．癌細胞は宿主免疫から逃れ，循環の物理的負荷に耐える必要がある．時として癌細胞は塞栓を形成し，その生存率を上昇させている．癌細胞が転移先に到達すると，毛細血管に物理的に引っかかる，もしくは白血球の血管外流出に類似した機序で内皮細胞上で停止する．その機序にかかわる分子としては血管内皮細胞のセレクチンと，その受容体で白血球や癌細胞に発現するsialyl Lewis X, A(SLeX, SLeA)が知られている．その後インテグリンを介した安定型接着が生じるが，その際，血小板凝集も生着を助長していると考えられる．循環からの離脱には浸潤と類似した基質の分解と運動が必要と考えられる[4]．また，癌細胞は特定のケモカインレセプターを発現しており，転移先臓器が分泌するケモカインとの相互作用は臓器特異的転移機構を担っていると思われる．

大腸癌細胞の循環による移動，内皮細胞への付着，循環からの離脱

大腸癌組織におけるSLeAは予後因子として報告されており，同様の現象が生じている可能性がある．大腸癌においてはCXCR4などの高発現が報告されており，肝臓や肺に転移しやすいことの一因と考えられている．

4. 遠隔臓器における局所増殖

遠隔臓器における癌の増殖は循環からの離脱の前から既に再開していると考えられている．EMTを生じて遠隔臓器に到達した細胞はその多くが間葉上皮系移行(MET)というこれまでと逆の現象を起こして，原発巣と類似した形態を取るようになる．癌細胞の転移した部位は原発腫瘍内と同様に増殖可能な環境であるとは限らない．増殖可能な環境形成には血管新生など生理的な支援体制が必要である．それがない場合，転移巣は消滅するか微小転移として生存する[5]．

大腸癌の遠隔臓器における局所増殖

肝細胞から分泌されるIGFは大腸癌肝転移を促進すると報告されており，増殖可能な環境形成にかかわると思われる．また大腸癌細胞株におけるSMAD4欠損によるCCL15発現上昇が，MMP9を発現する骨髄由来の細胞を集積させ，転移巣の増殖にかかわると報告されている．これらの結果から，転移巣においても腫瘍細胞と環境を形成する細胞が協調してその増殖にかかわっていると考えられる．

おわりに

癌の浸潤，転移は古くから知られる悪性の指標である．その生物像は古くから研究者に興味を抱かせているが，転移が成立する過程は上述のごとく非常に複雑で成立する確率は非常に低い．よって一つ一つの過程を病理学や生物学的な手法を含めて検討する必要がある．その前提として全体を把握することが不可欠であり，その際の一助として本図説が読者に役立つことを願う．

文　献

1) 小嶋基寛，落合淳志：大腸癌の浸潤・転移に関連する分子(遺伝子異常，発現異常)．日本臨牀 **69**(増刊3)：149-152, 2011.
2) Ito TK, et al: Degradation of soluble VEGF receptor-1 by MMP allow VEGF access to endothelial cells. Blood **113**: 2123-2124, 2009.
3) Kojima M, et al: Elastic laminal invasion in colon cancer: diagnostic utility and histological features. Front Oncol **2**: 179, 2012.
4) Miles FL, et al: Stepping out of flow: capillary extravasation in cancer metastasis. Clin Exp Metastasis **25**: 305-324, 2008.
5) Weinberg RA: The Biology of Cancer. p587-654, Garland Science, Taylor & Fransis Group, LLC, Yew York, 2007.